Histological Scoring of Colitis and CAC

Tissue samples were fixed in 10% neutral-buffered formalin. For the assessment of colitis, paraffin-embedded sections (5 μm) were stained with hematoxylin and eosin (H&E). The sections were analyzed without prior knowledge of the type of treatments. The degree of inflammation in the colon was graded according to the previously described scoring system (2). Briefly, the presence of occasional inflammatory cells in the lamina propria was assigned a value of 0; increased numbers of inflammatory cells in the lamina propria a value 1, confluence of inflammatory cells, extending into the submucosa a value of 2, and transmural extension of the infiltrate a value of 3. For tissue damage, no mucosal damage was scored as 0; discrete lymphoepithelial lesions were scored as 1; surface mucosal erosion or focal ulceration was scored as 2; and extensive mucosal damage and extension into deeper structures of the bowel wall were scored as 3. The combined histological score ranged from 0 (no changes) to 6 (extensive cell infiltration and tissue damage). For CAC assessment, sections (5 μm) were cut stepwise (200 μm) through the complete block and stained with H&E. Tumor counts were performed in a blinded fashion.

Immunohistochemistry

Colon samples for immunohistochemistry were embedded into OCT compound, snap-frozen in liquid nitrogen, and stored at −80°C. Cryosections (7 μm) were fixed in 4% paraformaldehyde for 10 min and incubated with 3% hydrogen peroxide for 15 min at room temperature. The sections were blocked with 1% BSA for 60 min and then incubated with either anti-mouse TNF-α MAb (BD Biosciences, Franklin Lakes, NJ), anti-mouse CD4 MAb (BD Biosciences), anti-mouse F4/80 MAb (eBioscience, San Diego, CA), or isotype-matched control Ig (BD Biosciences), at 4°C overnight followed by incubation with goat anti-rat Ig (Histofine Simple Stain MAX-PO, Nichirei Biosciences, Tokyo, Japan), for 30 min. The signals were visualized by diaminobenzidine (peroxidase substrate kit, Vector Laboratories, Burlingame, CA) and the sections were counterstained with hematoxylin. For immunofluorescence studies, the sections were stained with anti-β-catenin MAb (BD Biosciences) or anti-p-p65 PAb at serine 276 (Cell Signaling Technology) followed by incubation with Alexa^{594}-conjugated anti-mouse IgG1 or anti-rabbit IgG (Invitrogen) and DAPI (Vector Laboratory).

Statistical Analysis

Results were expressed as means ± SE. Statistics were determined by nonparametric Mann-Whitney *U*-test, and *P* values <0.05 were considered significant.

RESULTS

TNF-α Is Markedly Upregulated in the Inflamed Mucosa of DSS-Treated Mice

To first assess whether TNF-α is induced in the inflamed colonic tissue in C57BL/6 mice by administration of DSS, mice were administered 3.0% DSS-contained drinking water for 5 days (*days 0* to *5*, acute phase) followed by removal of DSS for another 2–5 days (recovery phase) with preinjection with AOM 7 days before starting DSS treatment (Fig. 1*A*). Total RNA was then isolated from the colon tissues of these mice. Consistent with previous report (37), we observed significantly increased level of TNF-α mRNA at *days 7* and *10* in DSS-treated mice compared with the control preinjected with AOM without DSS treatment (Fig. 1*B*). This observation was also confirmed by Western blotting (data not shown). Furthermore, immunohistochemistry revealed that the majority of TNF-α-expressing cells were located in the lamina propria and

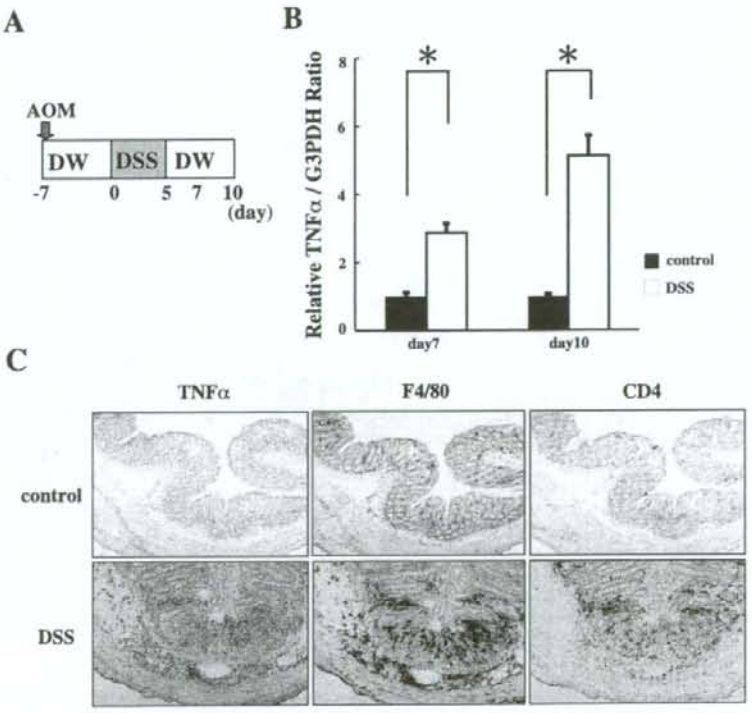

Fig. 1. TNF-α is profoundly induced in dextran sodium sulfate (DSS) colitis. *A*: protocol for acute DSS colitis. Mice were preinjected with 10 mg/kg of azoxymethane (AOM) or vehicle control 7 days before the start of DSS administration. DW, distilled water. *B*: relative mRNA expression of TNF-α in whole colon tissues that were taken from mice treated with control (regular water) or DSS at *days 7* and *10*. The levels of the mRNA were quantified by real-time PCR and normalized to the level of glyceraldehyde-3-phosphate dehydrogenase (G3PDH) ($n = 3$). *$P <$ 0.01. *C*: Immunohistochemistry. Frozen sections of colon tissues from control or DSS-treated mice at *day 10* were stained with anti-TNF-α, anti-CD4 or anti-F4/80 antibodies.

submucosa and some in the tunica muscularis (Fig. 1*C*). In addition, such TNF-α upregulation in DSS-treated colitis was not affected regardless of AOM preinjection (data not shown). Immunohistochemistry also revealed that the injured colonic tissues during the recovery phase were profoundly infiltrated by F4/80$^+$ macrophages as well as CD4$^+$ T cells compared with the untreated mice. Interestingly, the majority of TNF-α-expressing cells seemed to be macrophages rather than T cells (Fig. 1*C*). These results are consistent with the previous studies using BALB/c mice (37).

Administration of DSS Leads to Upregulation of TNFR2 but not TNFR1 in Colonic Epithelia

TNF-α-specific receptors composed of TNFR1 (p55) and 2 (p75) are known to be expressed in human intestinal epithelial cells and can be upregulated by IFN-γ (45, 49). Furthermore, it has been suggested that TNF-α is involved in the tissue repair of wounded epithelial layer (10). On the basis of the induction of TNF-α in colonic tissues by DSS treatment, TNFR1 and 2 protein expressions in colonic epithelial cells were predicted to be upregulated in this model. Therefore, we next assessed the expression levels of these molecules in the inflamed epithelial cells of AOM/DSS-treated mice. Primary colonic epithelial cells were isolated from the AOM-preinjected mice with or without DSS treatment described above at *day 10* (Fig. 1*A*). As expected, quantitative RT-PCR (Fig. 2*A*) and Western blotting (Fig. 2*B*) showed that colonic epithelial cells expressed endogenous low amount of both TNFR1 and 2. Notably, such expression of TNFR2, but not TNFR1, was significantly upregulated by DSS treatment (Fig. 2).

NF-κB Pathway, but not Death Domain Cascade, in Colonic Epithelial Cells Is Activated by DSS Treatment

It is suggested that the binding of TNF-α to TNFRs potentially results in the activation of two independent pathways, NF-κB and death domain (DD) (48). Given the result of TNFR2 upregulation in DSS colitis, we next assessed the activities of NF-κB and DD pathways in primary colonic epithelial cells from AOM/DSS-treated mice. As depicted in Fig. 3*A*, IκBα, which is upstream molecule of NF-κB, and p65/Rel A, one of the NF-κB components, were significantly activated in association with TNFR2 upregulation in AOM/DSS-treated colonic epithelia at *day 10*. In contrast, such treatment did not affect the expression of neither p-FADD nor cleaved (c)-caspase 3, a downstream molecule of DD, in these cells during the recovery phase (Fig. 3*B*).

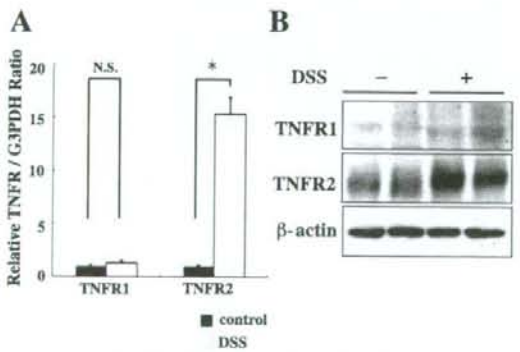

Fig. 2. TNF receptor (TNFR) 2 in colonic epithelia is upregulated in DSS colitis. *A*: relative mRNA expression levels of TNFR1 and 2 in colonic epithelial cells from mice treated with control (regular water) or DSS at *day 10*. The levels of the mRNAs were quantified by real-time PCR and normalized to the level of G3PDH ($n = 3$). *$P < 0.01$. *B*: protein lysates of isolated colonic epithelial cells from control- or DSS-treated mice at *day 10* were subjected to Western blotting with anti-TNFR1, anti-TNFR2, or anti-β-actin antibodies.

TNF-α Stimulates NF-κB Pathway in Intestinal Epithelial Cells

Given the upregulation of TNFR2 and specific activation of NF-κB, but not DD, in colonic epithelial cells in AOM/DSS colitis, we next utilized a mouse colonic epithelial cell line, CT26, to examine whether TNFR2 signaling is associated with NF-κB activation in these epithelial cells. CT26 cells were cultivated in the absence or presence of rIFN-γ to induce TNFRs upregulation. Although CT26 cells endogenously expressed TNFR2, its level was not upregulated in the presence of IFN-γ. This suggested that CT26 cells constitutively express maximum level of TNFR2 in the condition (data not shown). Moreover, we also observed that these cells express both p65 and IκBα (Fig. 4*A*). To further confirm whether TNFR2 in those cells is functional, the activation of NF-κB by rTNF-α was examined. Intestinal CT26 cells were stimulated with several concentrations of rTNF-α for 5 min. As shown in Fig. 4*A*, in vitro stimulation with rTNF-α led to the phosphorylation of p65 and IκBα in CT26 cells in a dose-dependent fashion.

Given the upregulated expression of TNFR2 and its signal profile in the stimulated-CT26 cells, we next examined the effect of anti-TNF-α MAb on NF-κB activation in these cells. CT26 cells were stimulated with 10 ng/ml of rTNF-α for 5 min in the presence of various concentrations of anti-TNF-α MAb, MP6-XT22. Although total expression level of p65 in rTNF-α-stimulated CT26 cells were not affected, phosphorylation of p65 in these cells was suppressed by the blockade of TNF-α with MP6-XT22 in a dose-dependent fashion (Fig. 4*B*). Similarly, neutralization of rTNF-α by MP6-XT22 also attenuated the phosphorylation status of IκBα in CT26 cells in a dose-dependent fashion. Furthermore, our kinetic assessment revealed that such suppression of NF-κB pathway by anti-TNF-α MAb did not express delayed signal response since both MP6-XT22-treated and control IgG-treated cells showed maximum level of p-p65 and p-IκBα around 10 min after the stimulation with rTNF-α (Fig. 4*C*). It should be noted that we consistently observed the degradation of IκBα 15 min after rTNF-α stimulation although the expressions of p-p65 and p-IκBα reach maximum level at 10 min. These results indicate that TNF-α stimulation against colonic epithelial cells results in activation of NF-κB via TNFR2 and, moreover, MP6-XT22 can arrest such activation.

Anti-TNF-α MAb Treatment Suppresses NF-κB Activation in Acute DSS Colitis Model

On the basis of the in vitro evidence of NF-κB inactivation by MP6-XT22 in rTNF-α-stimulated CT26 cells, we next confirmed this observation in the acute DSS colitis model to pursue more physiological function of MP6-XT22 in vivo. Because NF-κB is known to be critical in the induction of tissue inflammation such as colitis, it was initially anticipated that treatment with anti-TNF-α MAb would suppress the de-

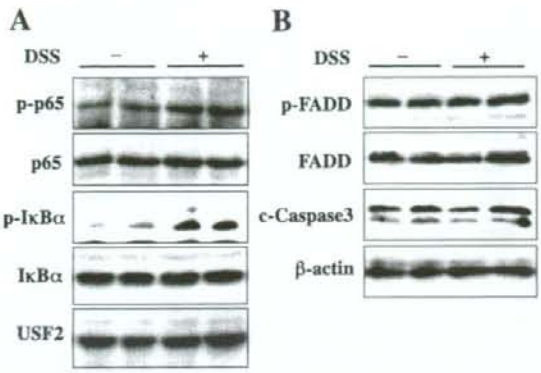

Fig. 3. NF-κB pathway in colonic epithelial cells is activated in DSS colitis. Protein lysates of isolated colonic epithelial cells from control or DSS-treated mice at *day 10* were subjected to Western blotting with either anti-p65, anti-p-p65, anti-IκBα, anti-p-IκBα, or anti-USF2 antibodies for the assessment of NF-κB activity (*A*) and anti-FADD, anti-p-FADD, anti-cleaved (c)-caspase 3, or anti-β-actin antibodies for apoptosis activity (*B*).

velopment of colitis. Therefore, we administered either control IgG or MP6-XT22 ip to the AOM/DSS-administered mice at *day 5* after DSS ingestion (Fig. 5*A*) followed by histological assessment at *days 7* and *10*. Then colonic epithelial cells were isolated at *day 10*. Unexpectedly, however, there was no significant difference in the histological score between two groups irrespective of administration of anti-TNF-α MAb or control IgG (Fig. 5*B*). On the other hand, AOM/DSS-treated epithelial samples with control IgG showed markedly upregulated p-IκBα and p-p65 expressions. However, injection with MP6-XT22 into AOM/DSS-treated mice resulted in suppression of IκBα and p65 phosphorylation, although total expression levels of p65 and IκBα were not affected in these samples (Fig. 5*C*). Given this discrepancy between the activities of NF-κB and the proportions of colitis in our experiments, we subsequently evaluated cytokine production such as IL-1β, IL-6, and MIP-2 (mouse homolog of human IL-8) in this model. Total RNA samples were extracted from colonic tissues of mice treated as above. Interestingly, quantitative RT-PCR analysis revealed significantly reduced mRNA expressions for IL-1β, IL-6, and MIP-2 in whole colons from MP6-XT22-treated mice at *day 7* compared with those of the control group (Fig. 5*D*). These results indicate that induced TNF-α in mucosal tissues may not be essential for colitis exacerbation but is somehow responsible for the production of these cytokine secondary to NF-κB activation in the DSS model.

Repetitive Anti-TNF-α MAb Treatment Suppresses Development of CAC in AOM/DSS-Treated Mice

The present protocol of anti-TNF-α MAb (MP6-XT22) administration has been useful in the assessment of TNF-α/TNFR signaling pathway on the development of CAC, because this does not affect the inflammation of DSS colitis but rather

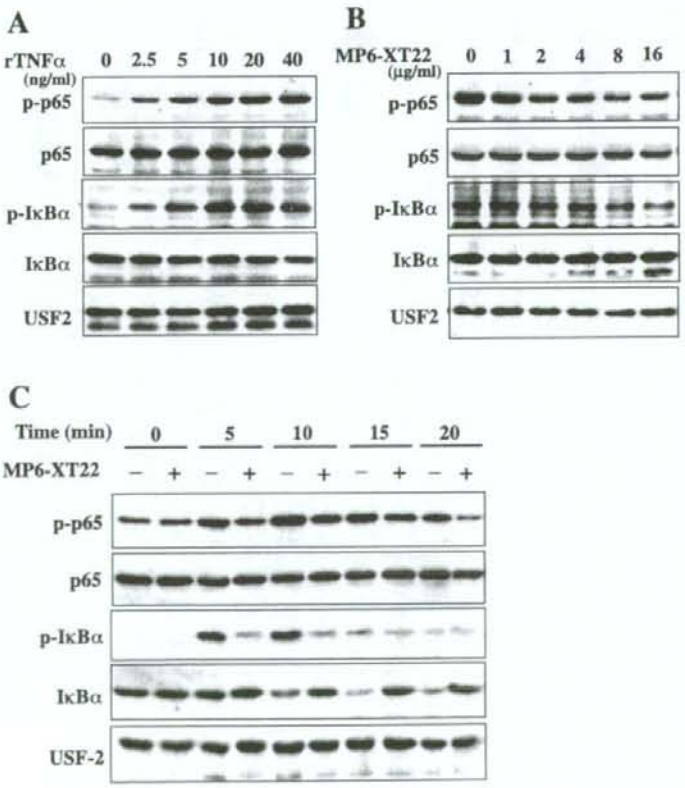

Fig. 4. MP6-XT22 suppresses NF-κB activation in TNF-α-stimulated CT26 cells. *A*: protein lysates from CT26 cells stimulated with indicated concentration of rTNF-α were subjected to Western blotting with anti-p65, anti-p-p65, anti-IκBα, anti-p-IκBα, or anti-USF2 antibodies. Representative data at 5 min after TNF-α-stimulation are shown. *B*: protein lysates from 10 ng/ml rTNF-α-stimulated CT26 cells incubated with the indicated concentration of MP6-XT22 were subjected to Western blotting with anti-p65, anti-p-p65 anti-IκBα, anti-p-IκBα, or anti-USF2 antibodies. Representative data at 5 min after TNF-α-stimulation are shown. *C*: protein lysates from CT26 cells incubated with either control IgG or MP6-XT22 (10 μg/ml) with rTNF-α (10 ng/ml) stimulation at the indicated time point were subjected to Western blotting with anti-p65, anti-p-p65 anti-IκBα, anti-p-IκBα, or anti-USF2 antibodies.

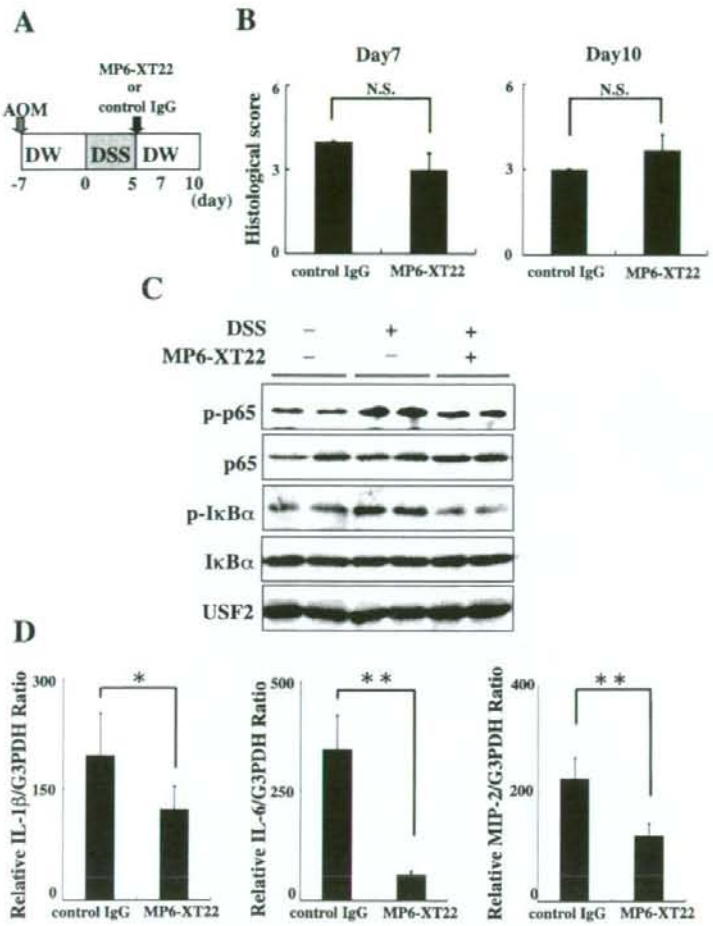

Fig. 5. MP6-XT22 treatment diminishes NF-κB activity in DSS-treated colonic epithelial cells, but it does not ameliorate severity of colitis. *A*: protocol for acute DSS colitis. Mice received MP6-XT22 or control IgG (1 mg/mouse) at *day 5*. *B*: histological scores at *day 7* ($n = 3$) and *day 10* ($n = 6$) are shown. Data are expressed as means ± SE. *C*: protein lysates of isolated colonic epithelial cells from control or DSS-treated mice at *day 10* with or without MP6-XT22 injection were subjected to Western blotting with anti-IκBα, anti-p-IκBα, anti-p65, anti-p-p65, or anti-USF2 antibodies. *D*: relative mRNA expressions for IL-1β, IL-6 and MIP-2 in whole colons from mice treated with control IgG or MP6-XT22 injection at *day 10*. Each mRNA level was quantified by real-time PCR and normalized to the level of G3PDH ($n = 3$). $^{*}P < 0.01$, $^{**}P < 0.05$.

suppress activation of NF-κB in epithelial cells. Therefore, this excludes the possibility that different degree of inflammation by the treatment secondarily affect the development of CAC. Thus we next investigated whether repetitive administration anti-TNF-α MAb suppresses the development of CAC in AOM/DSS-treated mice. Mice received AOM IP at *day −7*, followed by three cycles of DSS treatment and weekly injection of either control IgG or MP6-XT22 from *day 5* until *day 68*. These mice were then euthanized on *day 70* (see Fig. 6*A*). Consistent with acute model of DSS colitis as mentioned above, both groups of mice showed similar severity of clinical phenotypes as determined by weight loss, rectal bleeding, and diarrhea regardless of the treatments with MP6-XT22 (Fig. 6*B*). Histological findings of crypt destruction, mucosal ulceration, and infiltration were similarly observed in both groups of mice in association with the clinical scores of these mice (Fig. 6*C*). It should be noted that clinical and histological scores showed that the severity of inflammation was not affected by AOM treatment (data not shown).

It has been recently reported that NF-κB activation in epithelial cells and myeloid cells plays a crucial role in carcinogenesis (12). Thus it was suggested that blockade of TNF-α may be effective for incidence and/or progression of tumors. Therefore, we investigated the effect of anti-TNF-α MAb on the development of colitis-associated tumors in chronic DSS/AOM model. Mice administered with combination of AOM, DSS, and control IgG showed development of multiple nodular or polyploid tumors in the middle to distal colon (Fig. 7*A*). In contrast, decreased number of tumors was observed in mice administered with the combination of AOM, DSS, and MP6-XT22 (Fig. 7, *A* and *B*). Moreover, MP6-XT22 treatment also decreased the numbers of small tumors as well as larger tumors (Fig. 7*C*), despite similar morphological diversity in both groups (Fig. 7*D*), suggesting that the suppressed tumorigenesis in MP6-XT22-treated group is not only due to the reduced progression of tumors. Next, we thoroughly examined the histological sections, and no evidence of carcinoma such as tumor invasion into the lamina propria was observed in both control IgG and MP6-XT22 treated groups. Therefore, we defined the histology of this colitis-associated tumor model as adenoma. In addition, we also examined the β-catenin expression in these sections. The expression of β-catenin was observed in the cytoplasm, but not in the nuclei, of intestinal epithelia with colitis, as seen in Fig. 7*E*. However, the tumor

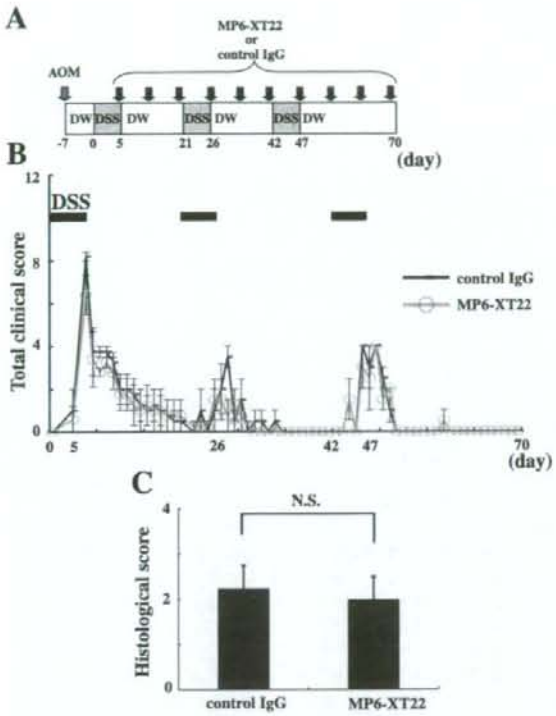

Fig. 6. MP6-XT22 does not ameliorate chronic DSS colitis. *A*: schema of the AOM/DSS colitis-associated tumor model. Mice were preinjected with AOM 7 days before starting DSS administration, and subsequently administered weekly injections of MP6-XT22 or isotype control from *day 5* until day 68 during the three cycles of DSS administration. *B* and *C*: clinical (*B*) and histological (*C*) scores are shown. Data (n = 10) are expressed as means ± SE. N.S., not significant.

cells showed the nuclear expression of β-catenin as well as its overexpression in the cytoplasm (Fig. 7*E*). Given the nuclear translocation of β-catenin in our tumor model (Fig. 7*E*) and the attenuation of tumor development by anti-TNF-α therapy (Fig. 7, *A–C*), we next examined TNFR2 expression as well as NF-κB activities in this model. Interestingly, TNFR2 expression was more upregulated in the colitis-associated tumor. In addition, the phosphorylation of IκBα and p65 was further induced in the tumors in association with the upregulation of TNFR2 (Fig. 7*F*). These studies indicate that the NF-κB activation via TNFR2 in intestinal epithelial cells is closely associated with epithelial tumorigenesis. Moreover, we also observed that the nuclear expression of p65 was induced in the epithelia in tumor

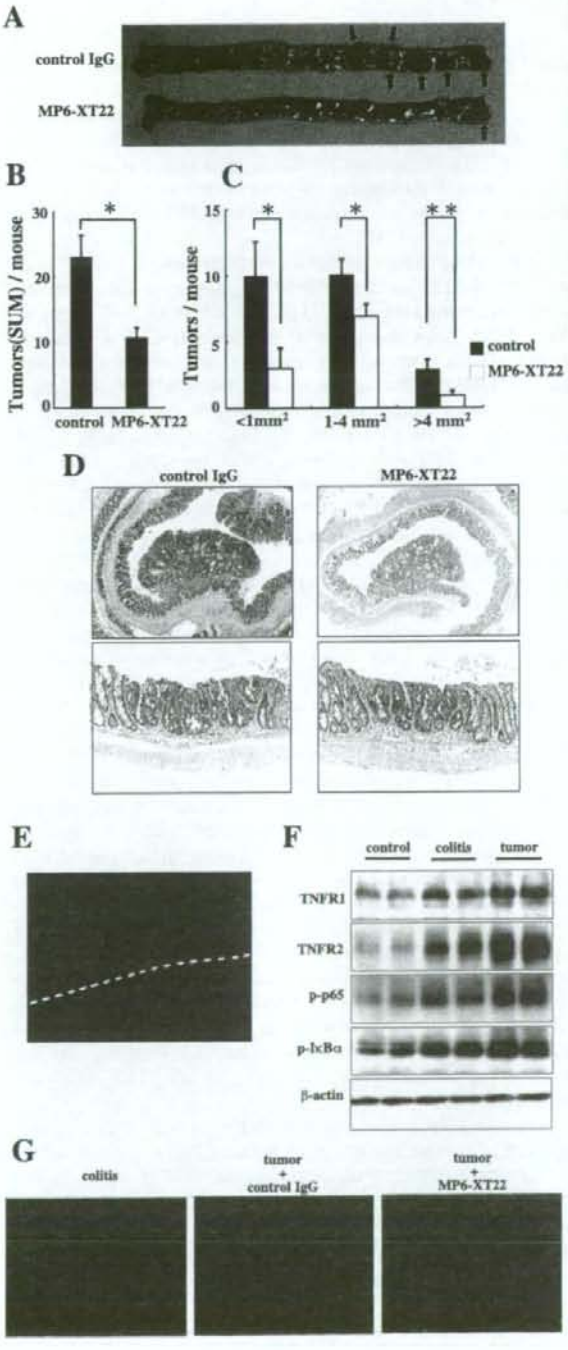

Fig. 7. MP6-XT22 reduces tumor development in AOM/DSS model. *A*: macroscopic overview of representative colonic samples from each group is shown. Arrows indicate tumors. *B*: numbers of microscopically indicated tumors per colon in AOM/DSS-administered mice with isotype control or MP6-XT22 treatment (n = 10). Data are express as means ± SE. $^*P < 0.01$, $^{**}P < 0.05$. *C*: histogram shows tumor size distribution. Tumors were determined under the microscope. *D*: microscopic morphology of AOM/DSS tumor model. Representative histological sections with hematoxylin and eosin staining from each group are shown. *E*: β-catenin expression in colitis-associated cancer (CAC). Cryosections from AOM/DSS-treated mice were stained with anti-β-catenin MAb and anti-mouse IgG1-Alexa^{594}. Representative sample at *day 70* is shown. *Top*, tumor area; *bottom*, nontumor area. *F*: protein lysates of isolated epithelial cells from nontreated control, colitis or tumor tissues were subjected to Western blotting with anti-TNFR1, anti-TNFR2, anti-p-p65, anti-p-IκBα or anti-β-actin antibodies. *G*: cryosections of colon tissues of healthy control, colitis, CAC with control IgG or CAC with MP6-XT22 treatment were stained with anti-p-p65 PAb and anti-rabbit IgG-Alexa^{594}.

tissues. However, such nuclear translocation of p65 was significantly suppressed by MP6-XT22 treatment (Fig. 7*G*). These findings indicate that blockade of TNF-α may contribute to suppressed initiation of colitis-associated tumors in our AOM/DSS model as well as reduction of tumor progression.

DISCUSSION

Our studies showed that blockade of TNF-α in vivo did not affect the severity of DSS-induced inflammation but rather reduced the development and progression of CAC. It has been recently reported by another group that reduced inflammation in TNFR1-deficient mice may contribute to the suppression of CAC (37). However, our results suggest that continuous suppression of TNF-α activity by MAb injection for patients with IBD, even if they are refractory to anti-TNF-α therapy, may reduce the risk of CAC.

TNF-α is a pivotal cytokine in the pathogenesis of IBD since anti-TNF-α MAb therapy is used as a powerful and promising treatment for patients with CD (13, 41, 44) or UC (40) in recent years. It has been also reported that the anti-TNF-α treatment is also effective therapy in several animal models of colitis such as TNBS colitis model, $CD4^+CD45RB^{high}$ T cell-reconstituted model, bone marrow transplanted tgε 26 model, and Cottontop tamarin model (24, 30, 38). Interestingly, however, the effect of TNF-α MAb therapy is controversial in the DSS colitis model, which is an epithelial damage model rather than a T cell-mediated model. For example, it has been reported that anti-TNF-α antibody treatment can ameliorate acute and chronic DSS-induced colitis (20, 28). Moreover, multiple injections of anti-TNF-α Ab during the process of chronic DSS reduced the disease activity and cytokine productions in the first two cycles although adverse effects were observed in the third cycle of the DSS treatment (27). However, other groups have reported that the antibody therapy against TNF-α failed to suppress the severity of colitis in this model (20, 33). Moreover, it has been reported that DSS-induced inflammation was significantly enhanced in TNF-α deficient-animals (29). This observation is somewhat similar to our results since anti-TNF-α treatment did not affect the clinical symptoms and pathological studies. Since the wounded epithelial layer by DSS treatment results in the translocation of luminal bacteria into the intestinal mucosa in this model, one of the potential interpretations regarding the different observations by others and ours is that in the setting of inflammation in acute and/or chronic DSS colitis, environmental effect such as the different microflora in different animal facilities may explain the discrepancy among the above results. Another interpretation might be that the colitis model in our studies was relatively mild compared with the others' and therefore we did not observe explicit abrogation of colitis by anti-TNF MAb administration.

Secreted TNF-α molecules in inflamed tissues can be recognized by its specific receptors such as TNFR1 and 2, which are known to be expressed in several cell types including macrophages and intestinal epithelial cells. The cytoplasmic domains of TNFR1 and 2 are known to be associated with TRAF2 by which activation of IKK is induced. Subsequently, activated IKK induces phosphorylation of IκB, resulting in activation of NF-κB, which consists of p50 and Rel A/p65, due to dissociation of IκB/NF-κB complex. In addition to NF-κB activation, however, TNFR1 is also capable of being recruited by FADD and TNFR-associated DD protein (TRADD) by TNF-α activation. The oligomerization of such molecules induces activation of cysteine proteases such as caspase 8, resulting in apoptosis. Interestingly, however, TNFR2, which is not coupled with FADD/TRADD complex, does not induce proapoptotic signaling when interacting with TNF-α. In this regard, we observed that TNFR2 is preferentially upregulated in regenerating epithelial cells in DSS colitis. Our interpretation of these results are that intestinal epithelial cells, when rapidly expanding, is associated with the expression of TNFR2 rather than TNFR1, and thus counter that of the proapoptotic signals of intestinal epithelia. Consistent with this, we also observed specific activation of IκB and p65 in association with TNFR2 upregulation in wounded mucosal epithelia by DSS administration. Thus it is suggested that regenerating intestinal epithelial cells may have susceptibility of NF-κB inactivation by blockade of TNF-α due to the specific upregulation of TNFR2 in these cells.

It is well known that long-standing UC (8, 18, 25) and CD (4, 7) are closely associated with an increased risk of CAC. To investigate the role of TNF-α signaling in colon carcinogenesis, we here used an established murine CAC model based on the mutagenic agent AOM (32, 43) along with the colitogenic administration of DSS. It has been suggested by Greten and colleagues (12) that IKK-β contributes to tumor promotion in AOM/DSS-induced CAC model. They indicated that the deletion of IKK-β in myeloid cells or epithelial cells resulted in decreased size of tumors due to reduced expression of proinflammatory cytokines that may serve as tumor growth factors (12). Moreover, it has been reported that blockade of IL-6 prevents tumor progression in AOM/DSS-induced CAC model (3). In addition, Popivanova and colleagues (37) have recently reported that the TNFR1 signaling in hematopoietic cells in colonic tissues results in production of chemokines such as CXCL1 and CCL2, which are chemotactic for neutrophils and macrophages. They also suggested that such activation of hematopoietic cells in the mucosal tissue is critical for the progression of CAC in association with suppression of DSS colitis. In our studies, colitis was mild and not clearly affected by anti-TNF-α MAb treatment despite the depressed CAC initiation and progression observed. One of the interpretations regarding different observations is that TNFR1 deficient neutrophils and macrophages on the BALB/c background may have different immunological context from that of our model on the C57BL/6 background. Some of our observation is consistent with these, because blockade of TNF-α in chronic DSS colitis by treatment with MP6-XT22 resulted in decreased cytokine expression including IL-1β, IL-6, and MIP-2, which are considered to encourage protumorigenic activities such as angiogenesis and tumor proliferation (5, 6, 19, 21). Thus it is suggested that the blockade of TNF-α may function to suppress the secretion of these chemokines and cytokines from infiltrating lymphocytes in colitic tissue through the inhibition of NK-κB activity in these cells. It should be noted that anti-TNF-α MAb treatment is also effective for suppression of tumorigenesis in unique mouse CAC model, which is promoted by transferring of $CD4^+CD45RB^{high}$ lymphocytes that may produce proinflammatory cytokine into Apc (Min/+) mice (39). This might be another evidence for the proinflammatory cytokine-induced epithelial carcinogenesis.

On the other hand, it was also suggested by Greten and colleagues (12) that deletion of IKK-β in intestinal epithelial cells led to a decrease in tumor incidence although inflammation in the tissue was not abrogated. Consistent with this, it was also suggested by another group that inactivation of NF-κB in the hepatocytes had no effect during the course of hepatitis but failed to progress to carcinoma in an animal model of hepatitis-induced hepatocellular carcinoma (36). Although the amelioration of colitis was not apparent in our study, anti-TNF-α Ab significantly suppressed the tumor development in our AOM/DSS model in association with the downregulation of p-p65 and p-IκB. Thus our results are consistent with observations by others above since treatment with MP6-XT22 resulted in the reduction of TNF-α-induced NF-κB activity in colonic epithelial cells, which may influence the cell growth of colonic epithelia in DSS colitis. Regarding the involvement of apoptosis, we have tried to detect p-FADD and c-caspase 3 expressions in DSS-receiving mice, but we did not observe any significant differences compared with nontreated controls, as seen in Fig. 3*B*. Moreover, we have also tried to detect DNA fragmentation from rTNF-α-stimulated CT26 cells as well as TUNEL staining in the setting of recovery phase of DSS-treated or AOM/DSS-treated mice with or without anti-TNF-α treatment. However, we were not able to observe any significant difference of apoptosis activities in these experiments compared with the controls (data not shown). Therefore, we conclude that apoptosis is unlikely to be associated with the development of our colitis-associated tumor model. Moreover, we have also observed that the NF-κB pathway is further activated in CAC tissues compared with nontumor tissues in DSS/AOM-receiving mice in association with nuclear expression of β-catenin (Fig. 7*E*) and extraordinary upregulation of TNFR2 (Fig. 7*F*). These observations evidently imply that NF-κB activation via TNFR2 in the intestinal epithelial cells is directly correlated with the carcinogenesis induced by TNF-α stimulation. Thus it should be clarified that TNFR2 signaling in intestinal epithelia is also required for such tumor promotion as well as TNFR1 signaling in hematopoietic cells. We have therefore tried to focus on addressing this issue by using a "conventional" TNFR2-deficient model. We administered AOM and DSS treatment to these mice; however, we were not able to quantify and compare tumor development in such mice, because these mice were more sensitive to DSS colitis and had higher mortality compared with WT mice (data not shown). Our interpretation of this result is that serum TNF-α levels in conventional TNFR2-deficient mice may be elevated with LPS stimulation as previously reported by other group (35). We therefore realized that an "intestinal epithelia-specific" deficient model rather than conventional knockout mice would likely be the better model for our study. However, we were not able to obtain such conditional deficient mice. On the other hand, Fukata and colleagues (11) have recently reported that impaired Toll-like receptor-4 (TLR4) signaling reduced AOM/DSS-induced colon cancer without significant impact on inflammation. Their findings and ours may imply an important mechanism by which NF-κB pathway is regulated in intestinal epithelial cells in setting of carcinogenesis. Thus one potential mechanism by which anti-TNF-α MAb is able to reduce the numbers and size of tumors in AOM/DSS-administered mice is that blocking TNFR2 signaling, which was presumably triggered by TLR4-mediated epithelial stimulation, in the context of chronic intestinal wound healing may somehow decrease neoplasia even without significantly impairing inflammation. In addition, we have also observed that TNFR2 signaling in colonic epithelial cells results in the epithelial barrier dysfunction (M. Onizawa and T. Nagaishi, unpublished data). This observation suggests that TNFR2 signaling-mediated impairment of epithelial tight junction may be associated with the mechanism of tumor development.

In summary, administration of anti-TNF-α MAb directly inhibits NF-κB activities in intestinal epithelial cells that may induce tumor formation in collaboration with independent mechanisms by another NF-κB activity in the hematopoietic cells. Although more detail mechanism still remains to be elucidated, distinct TNF-α signaling in colonic epithelial cells may be one potential therapeutic target in the treatment of IBD-associated tumorigenesis, resulting in the change of natural history of patients with IBD.

ACKNOWLEDGMENTS

The authors thank Drs. Emiko Mizoguchi and Timothy Kuo for helpful discussions on this study.

GRANTS

This study was supported in part by grants-in-aid for Scientific Research, Scientific Research on Priority Areas, Exploratory Research and Creative Scientific Research from the Japanese Ministry of Education, Culture, Sports, Science and Technology; the Japanese Ministry of Health, Labor and Welfare; the Japan Medical Association; Foundation for Advancement of International Science; Terumo Life Science Foundation; Ohyama Health Foundation; Yakult Bio-Science Foundation; Research Fund of Mitsukoshi Health and Welfare Foundation; Japan Foundation for Applied Enzymology; Memorial Fund of Nihon University Medical Alumni Association; Abbott Japan Allergy Research Award; and Takeda Science Foundation.

REFERENCES

1. **Abrams JS, Roncarolo MG, Yssel H, Andersson U, Gleich GJ, Silver JE.** Strategies of anti-cytokine monoclonal antibody development: immunoassay of IL-10 and IL-5 in clinical samples. *Immunol Rev* 127: 5–24, 1992.
2. **Araki A, Kanai T, Ishikura T, Makita S, Uraushihara K, Iiyama R, Totsuka T, Takeda K, Akira S, Watanabe M.** MyD88-deficient mice develop severe intestinal inflammation in dextran sodium sulfate colitis. *J Gastroenterol* 40: 16–23, 2005.
3. **Becker C, Fantini MC, Schramm C, Lehr HA, Wirtz S, Nikolaev A, Burg J, Strand S, Kiesslich R, Huber S, Ito H, Nishimoto N, Yoshizaki K, Kishimoto T, Galle PR, Blessing M, Rose-John S, Neurath MF.** TGF-beta suppresses tumor progression in colon cancer by inhibition of IL-6 trans-signaling. *Immunity* 21: 491–501, 2004.
4. **Bernstein CN, Blanchard JF, Kliewer E, Wajda A.** Cancer risk in patients with inflammatory bowel disease: a population-based study. *Cancer* 91: 854–862, 2001.
5. **Coussens LM, Werb Z.** Inflammation and cancer. *Nature* 420: 860–867, 2002.
6. **Driscoll KE, Hassenbein DG, Howard BW, Isfort RJ, Cody D, Tindal MH, Suchanek M, Carter JM.** Cloning, expression, and functional characterization of rat MIP-2: a neutrophil chemoattractant and epithelial cell mitogen. *J Leukoc Biol* 58: 359–364, 1995.
7. **Ekbom A, Helmick C, Zack M, Adami HO.** Increased risk of large-bowel cancer in Crohn's disease with colonic involvement. *Lancet* 336: 357–359, 1990.
8. **Ekbom A, Helmick C, Zack M, Adami HO.** Ulcerative colitis and colorectal cancer. A population-based study. *N Engl J Med* 323: 1228–1233, 1990.
9. **Ekbom A, Helmick CG, Zack M, Holmberg L, Adami HO.** Survival and causes of death in patients with inflammatory bowel disease: a population-based study. *Gastroenterology* 103: 954–960, 1992.
10. **Feiken E, Romer J, Eriksen J, Lund LR.** Neutrophils express tumor necrosis factor-alpha during mouse skin wound healing. *J Invest Dermatol* 105: 120–123, 1995.

11. **Fukata M, Chen A, Vamadevan AS, Cohen J, Breglio K, Krishnareddy S, Hsu D, Xu R, Harpaz N, Dannenberg AJ, Subbaramaiah K, Cooper HS, Itzkowitz SH, Abreu MT.** Toll-like receptor-4 promotes the development of colitis-associated colorectal tumors. *Gastroenterology* 133: 1869–1881, 2007.
12. **Greten FR, Eckmann L, Greten TF, Park JM, Li ZW, Egan LJ, Kagnoff MF, Karin M.** IKKbeta links inflammation and tumorigenesis in a mouse model of colitis-associated cancer. *Cell* 118: 285–296, 2004.
13. **Hanauer SB, Feagan BG, Lichtenstein GR, Mayer LF, Schreiber S, Colombel JF, Rachmilewitz D, Wolf DC, Olson A, Bao W, Rutgeerts P.** Maintenance infliximab for Crohn's disease: the ACCENT I randomised trial. *Lancet* 359: 1541–1549, 2002.
14. **Itzkowitz SH.** Cancer prevention in patients with inflammatory bowel disease. *Gastroenterol Clin North Am* 31: 1133–1144, 2002.
15. **Kanai T, Totsuka T, Uraushihara K, Makita S, Nakamura T, Koganei K, Fukushima T, Akiba H, Yagita H, Okumura K, Machida U, Iwai H, Azuma M, Chen L, Watanabe M.** Blockade of B7-H1 suppresses the development of chronic intestinal inflammation. *J Immunol* 171: 4156–4163, 2003.
16. **Karhausen J, Furuta GT, Tomaszewski JE, Johnson RS, Colgan SP, Haase VH.** Epithelial hypoxia-inducible factor-1 is protective in murine experimental colitis. *J Clin Invest* 114: 1098–1106, 2004.
17. **Karin M, Cao Y, Greten FR, Li ZW.** NF-kappaB in cancer: from innocent bystander to major culprit. *Nature Rev* 2: 301–310, 2002.
18. **Karlen P, Lofberg R, Brostrom O, Leijonmarck CE, Hellers G, Persson PG.** Increased risk of cancer in ulcerative colitis: a population-based cohort study. *Am J Gastroenterol* 94: 1047–1052, 1999.
19. **Koch AE, Polverini PJ, Kunkel SL, Harlow LA, DiPietro LA, Elner VM, Elner SG, Strieter RM.** Interleukin-8 as a macrophage-derived mediator of angiogenesis. *Science* 258: 1798–1801, 1992.
20. **Kojouharoff G, Hans W, Obermeier F, Mannel DN, Andus T, Scholmerich J, Gross V, Falk W.** Neutralization of tumour necrosis factor (TNF) but not of IL-1 reduces inflammation in chronic dextran sulphate sodium-induced colitis in mice. *Clin Exp Immunol* 107: 353–358, 1997.
21. **Lahm H, Petral-Malec D, Yilmaz-Ceyhan A, Fischer JR, Lorenzoni M, Givel JC, Odartchenko N.** Growth stimulation of a human colorectal carcinoma cell line by interleukin-1 and -6 and antagonistic effects of transforming growth factor beta 1. *Eur J Cancer* 28A: 1894–1899, 1992.
22. **Li Q, Verma IM.** NF-kappaB regulation in the immune system. *Nat Rev Immunol* 2: 725–734, 2002.
23. **MacDonald TT, Monteleone G, Pender SL.** Recent developments in the immunology of inflammatory bowel disease. *Scand J Immunol* 51: 2–9, 2000.
24. **Mackay F, Browning JL, Lawton P, Shah SA, Comiskey M, Bhan AK, Mizoguchi E, Terhorst C, Simpson SJ.** Both the lymphotoxin and tumor necrosis factor pathways are involved in experimental murine models of colitis. *Gastroenterology* 115: 1464–1475, 1998.
25. **Mellemkjaer L, Olsen JH, Frisch M, Johansen C, Gridley G, McLaughlin JK.** Cancer in patients with ulcerative colitis. *Int J Cancer* 60: 330–333, 1995.
26. **Moore RJ, Owens DM, Stamp G, Arnott C, Burke F, East N, Holdsworth H, Turner L, Rollins B, Pasparakis M, Kollias G, Balkwill F.** Mice deficient in tumor necrosis factor-alpha are resistant to skin carcinogenesis. *Nat Med* 5: 828–831, 1999.
27. **Murthy S, Cooper HS, Yoshitake H, Meyer C, Meyer CJ, Murthy NS.** Combination therapy of pentoxifylline and TNFalpha monoclonal antibody in dextran sulphate-induced mouse colitis. *Aliment Pharmacol Ther* 13: 251–260, 1999.
28. **Myers KJ, Murthy S, Flanigan A, Witchell DR, Butler M, Murray S, Siwkowski A, Goodfellow D, Madsen K, Baker B.** Antisense oligonucleotide blockade of tumor necrosis factor-alpha in two murine models of colitis. *J Pharmacol Exp Ther* 304: 411–424, 2003.
29. **Naito Y, Takagi T, Handa O, Ishikawa T, Nakagawa S, Yamaguchi T, Yoshida N, Minami M, Kita M, Imanishi J, Yoshikawa T.** Enhanced intestinal inflammation induced by dextran sulfate sodium in tumor necrosis factor-alpha deficient mice. *J Gastroenterol Hepatol* 18: 560–569, 2003.
30. **Neurath MF, Fuss I, Pasparakis M, Alexopoulou L, Haralambous S, Meyer zum Buschenfelde KH, Strober W, Kollias G.** Predominant pathogenic role of tumor necrosis factor in experimental colitis in mice. *Eur J Immunol* 27: 1743–1750, 1997.
31. **Nielsen OH, Vainer B, Madsen SM, Seidelin JB, Heegaard NH.** Established and emerging biological activity markers of inflammatory bowel disease. *Am J Gastroenterol* 95: 359–367, 2000.
32. **Okayasu I, Ohkusa T, Kajiura K, Kanno J, Sakamoto S.** Promotion of colorectal neoplasia in experimental murine ulcerative colitis. *Gut* 39: 87–92, 1996.
33. **Olson AD, DelBuono EA, Bitar KN, Remick DG.** Antiserum to tumor necrosis factor and failure to prevent murine colitis. *J Pediatr Gastroenterol Nutr* 21: 410–418, 1995.
34. **Oshima S, Nakamura T, Namiki S, Okada E, Tsuchiya K, Okamoto R, Yamazaki M, Yokota T, Aida M, Yamaguchi Y, Kanai T, Handa H, Watanabe M.** Interferon regulatory factor 1 (IRF-1) and IRF-2 distinctively up-regulate gene expression and production of interleukin-7 in human intestinal epithelial cells. *Mol Cell Biol* 24: 6298–6310, 2004.
35. **Peschon JJ, Torrance DS, Stocking KL, Glaccum MB, Otten C, Willis CR, Charrier K, Morrissey PJ, Ware CB, Mohler KM.** TNF receptor-deficient mice reveal divergent roles for p55 and p75 in several models of inflammation. *J Immunol* 160: 943–952, 1998.
36. **Pikarsky E, Porat RM, Stein I, Abramovitch R, Amit S, Kasem S, Gutkovich-Pyest E, Urieli-Shoval S, Galun E, Ben-Neriah Y.** NF-kappaB functions as a tumour promoter in inflammation-associated cancer. *Nature* 431: 461–466, 2004.
37. **Popivanova BK, Kitamura K, Wu Y, Kondo T, Kagaya T, Kaneko S, Oshima M, Fujii C, Mukaida N.** Blocking TNF-alpha in mice reduces colorectal carcinogenesis associated with chronic colitis. *J Clin Invest* 118: 560–570, 2008.
38. **Powrie F, Leach MW, Mauze S, Menon S, Caddle LB, Coffman RL.** Inhibition of Th1 responses prevents inflammatory bowel disease in scid mice reconstituted with CD45RBhi CD4+ T cells. *Immunity* 1: 553–562, 1994.
39. **Rao VP, Poutahidis T, Ge Z, Nambiar PR, Horwitz BH, Fox JG, Erdman SE.** Proinflammatory CD4+ CD45RB(hi) lymphocytes promote mammary and intestinal carcinogenesis in Apc(Min/+) mice. *Cancer Res* 66: 57–61, 2006.
40. **Rutgeerts P, Sandborn WJ, Feagan BG, Reinisch W, Olson A, Johanns J, Travers S, Rachmilewitz D, Hanauer SB, Lichtenstein GR, de Villiers WJ, Present D, Sands BE, Colombel JF.** Infliximab for induction and maintenance therapy for ulcerative colitis. *N Engl J Med* 353: 2462–2476, 2005.
41. **Sands BE, Anderson FH, Bernstein CN, Chey WY, Feagan BG, Fedorak RN, Kamm MA, Korzenik JR, Lashner BA, Onken JE, Rachmilewitz D, Rutgeerts P, Wild G, Wolf DC, Marsters PA, Travers SB, Blank MA, van Deventer SJ.** Infliximab maintenance therapy for fistulizing Crohn's disease. *N Engl J Med* 350: 876–885, 2004.
42. **Szlosarek P, Charles KA, Balkwill FR.** Tumour necrosis factor-alpha as a tumour promoter. *Eur J Cancer* 42: 745–750, 2006.
43. **Tanaka T, Kohno H, Suzuki R, Yamada Y, Sugie S, Mori H.** A novel inflammation-related mouse colon carcinogenesis model induced by azoxymethane and dextran sodium sulfate. *Cancer Sci* 94: 965–973, 2003.
44. **Targan SR, Hanauer SB, van Deventer SJ, Mayer L, Present DH, Braakman T, DeWoody KL, Schaible TF, Rutgeerts PJ.** A short-term study of chimeric monoclonal antibody cA2 to tumor necrosis factor alpha for Crohn's disease. Crohn's Disease cA2 Study Group. *N Engl J Med* 337: 1029–1035, 1997.
45. **Taylor CT, Dzus AL, Colgan SP.** Autocrine regulation of epithelial permeability by hypoxia: role for polarized release of tumor necrosis factor alpha. *Gastroenterology* 114: 657–668, 1998.
46. **Totsuka T, Kanai T, Iiyama R, Uraushihara K, Yamazaki M, Okamoto R, Hibi T, Tezuka K, Azuma M, Akiba H, Yagita H, Okumura K, Watanabe M.** Ameliorating effect of anti-inducible costimulator monoclonal antibody in a murine model of chronic colitis. *Gastroenterology* 124: 410–421, 2003.
47. **Totsuka T, Kanai T, Uraushihara K, Iiyama R, Yamazaki M, Akiba H, Yagita H, Okumura K, Watanabe M.** Therapeutic effect of anti-OX40L and anti-TNF-alpha MAbs in a murine model of chronic colitis. *Am J Physiol Gastrointest Liver Physiol* 284: G595–G603, 2003.
48. **Wajant H, Pfizenmaier K, Scheurich P.** Tumor necrosis factor signaling. *Cell Death Differ* 10: 45–65, 2003.
49. **Wang F, Schwarz BT, Graham WV, Wang Y, Su L, Clayburgh DR, Abraham C, Turner JR.** IFN-gamma-induced TNFR2 expression is required for TNF-dependent intestinal epithelial barrier dysfunction. *Gastroenterology* 131: 1153–1163, 2006.
50. **Wang M, Bronte V, Chen PW, Gritz L, Panicali D, Rosenberg SA, Restifo NP.** Active immunotherapy of cancer with a nonreplicating recombinant fowlpox virus encoding a model tumor-associated antigen. *J Immunol* 154: 4685–4692, 1995.

Am J Physiol Gastrointest Liver Physiol 296: G23–G35, 2009.
First published November 20, 2008; doi:10.1152/ajpgi.90225.2008.

Requirement of Notch activation during regeneration of the intestinal epithelia

Ryuichi Okamoto,[1,2] Kiichiro Tsuchiya,[2] Yasuhiro Nemoto,[2] Junko Akiyama,[2] Tetsuya Nakamura,[1,2] Takanori Kanai,[2] and Mamoru Watanabe[2]

[1]*Department of Advanced Therapeutics in Gastrointestinal Diseases and* [2]*Department of Gastroenterology and Hepatology, Graduate School, Tokyo Medical and Dental University, Tokyo, Japan*

Submitted 7 March 2008; accepted in final form 18 November 2008

Okamoto R, Tsuchiya K, Nemoto Y, Akiyama J, Nakamura T, Kanai T, Watanabe M. Requirement of Notch activation during regeneration of the intestinal epithelia. *Am J Physiol Gastrointest Liver Physiol* 296: G23–G35, 2009. First published November 20, 2008; doi:10.1152/ajpgi.90225.2008.—Notch signaling regulates cell differentiation and proliferation, contributing to the maintenance of diverse tissues including the intestinal epithelia. However, its role in tissue regeneration is less understood. Here, we show that Notch signaling is activated in a greater number of intestinal epithelial cells in the inflamed mucosa of colitis. Inhibition of Notch activation in vivo using a γ-secretase inhibitor resulted in a severe exacerbation of the colitis attributable to the loss of the regenerative response within the epithelial layer. Activation of Notch supported epithelial regeneration by suppressing goblet cell differentiation, but it also promoted cell proliferation, as shown in in vivo and in vitro studies. By utilizing tetracycline-dependent gene expression and microarray analysis, we identified a novel group of genes that are regulated downstream of Notch1 within intestinal epithelial cells, including PLA2G2A, an antimicrobial peptide secreted by Paneth cells. Finally, we show that these functions of activated Notch1 are present in the mucosa of ulcerative colitis, mediating cell proliferation, goblet cell depletion, and ectopic expression of PLA2G2A, thereby contributing to the regeneration of the damaged epithelia. This study showed the critical involvement of Notch signaling during intestinal tissue regeneration, regulating differentiation, proliferation, and antimicrobial response of the epithelial cells. Thus Notch signaling is a key intracellular molecular pathway for the proper reconstruction of the intestinal epithelia.

intestinal epithelial cells; goblet cells; PLA2G2A; ulcerative colitis

THE INTESTINAL EPITHELIA are composed of four lineages of intestinal epithelial cells (IECs) that arise from intestinal stem cells (1). Recent studies have shown that various signals such as Wnt, Sonic hedgehog, and bone morphogenetic protein interact within the stem and progenitor cells of the intestinal epithelia to finely regulate the expansion and the cell fate decision of IECs. Other studies have revealed that Notch signaling may also play critical roles in the maintenance of the intestinal epithelia (20).

Notch signaling is a signaling pathway known to regulate differentiation and proliferation of cells in diverse adult tissues (1). Activation of Notch receptor is mediated by the cleavage of its intracellular domain (NICD), and this intracellular domain translocates from the cell membrane to the nucleus, thereby functioning as a transcriptional activator of target genes such as Hes1 (10, 25). The functional role of Notch signaling in the intestine was first described in a study of Hes1-null mice; depletion of Hes1 was associated with significant increases in the secretory lineage IECs (9). Other studies have shown that the activation of Notch promoted proliferation of crypt progenitor cells and directed their cell fates toward absorptive but not secretory lineage cells (6, 28, 33). A recent study suggested that Notch might also function in postmitotic IECs, directing their cell fates toward secretory lineage cells (42). Thus these studies have suggested that Notch signaling functions in the intestine to regulate differentiation and proliferation of IECs, contributing to the maintenance and the homeostasis of the intestinal mucosa. However, the role of Notch signaling in tissue regeneration is less understood.

Damage of the intestinal epithelia is observed in a wide variety of diseases, such as acute intestinal infections, radiation injuries, or idiopathic inflammatory bowel diseases (23). Once the epithelial layer is damaged, it responds by restoring the continuity and integrated structure via activating the stepwise regeneration program (16). The initial response is called restitution, which is the redistribution of remaining IECs to rapidly cover the damaged area. This initial step is usually completed in an extremely short period of time and thus does not require the proliferation or expansion of IECs (19). However, in the next step, the rapid expansion of IECs is necessary to rebuild the proper structure of the epithelia. This response is manifested by the appearance of the regenerative epithelia in the intestine, showing a marked expansion of the proliferating compartment consisting of undifferentiated IECs. However, the exact molecular mechanisms involved in this critical step of intestinal epithelial regeneration has never been described.

Another change that is observed in the intestine during such a regenerative process is the ectopic expression of antimicrobial peptides by IECs. Paneth cells usually secrete peptides such as lysozymes, α-defensins, or PLA2G2A, and this helps to maintain the ideal environment for the stem and progenitor IECs within the small intestinal crypts. The ectopic expressions of these antimicrobial peptides by IECs are frequently observed in the inflamed colonic mucosa (5, 8), and such expressions likely support the local immune system in providing an ideal environment for the regeneration of the damaged mucosa.

In this study, we show that Notch signaling is activated in many IECs in the inflamed mucosa of murine colitis. Results show that the activation of Notch is critical for the proper regeneration program in the epithelial layer and that it helps to suppress goblet cell differentiation and promote cell proliferation. A comprehensive analysis identified a novel group of genes regulated by Notch in IECs, which included

Address for reprint requests and other correspondence: M. Watanabe, Dept. of Gastroenterology and Hepatology, Graduate School, Tokyo Medical and Dental Univ., 1-5-45 Yushima, Bunkyo-ku, Tokyo 113-8519, Japan (e-mail address: mamoru.gast@tmd.ac.jp).

The costs of publication of this article were defrayed in part by the payment of page charges. The article must therefore be hereby marked "*advertisement*" in accordance with 18 U.S.C. Section 1734 solely to indicate this fact.

a gene encoding an antimicrobial peptide called PLA2G2A. Such functions of Notch activation were present not only in the mice intestine but also in the human intestine. Finally, the clinical relevance of Notch-mediated regeneration is analyzed in ulcerative colitis (UC). Thus Notch signaling is a key-signaling pathway involved in intestinal tissue regeneration, in fine regulation of differentiation and proliferation, and in antimicrobial activities in IECs. Our findings point to a novel molecular target for agents that could promptly regenerate the intestinal mucosa in a wide range of intestinal diseases.

MATERIALS AND METHODS

Mice. C57BL/6J mice at 8 wk of age were purchased from Japan Clea. Mice were housed and maintained in the animal facility of Tokyo Medical and Dental University. The institutional animal use and care committee approved the study.

In vivo experiments. Induction of colitis was performed as previously described (17). Briefly, mice were fed ad libitum with 1.75% dextran sodium sulfate (DSS, Bio Research of Yokohama) for 5 consecutive days, followed by distilled water for another 5 days. For inhibition of Notch activation, mice were orally administered with either 5% DMSO (vehicle, VEC) or LY411,575 (LY) (10 mg/kg) dissolved in 0.5% (wt/vol) methylcellulose (WAKO), once daily for 5 consecutive days. Twenty-four mice were separated into four groups: *1*) fed distilled water for five days followed by daily administration of vehicle alone (VEC, $n = 6$) for 5 days, *2*) fed distilled water for 5 days followed by daily administration of LY411,575 (LY, $n = 6$) for five days, *3*) fed 1.75% DSS for 5 days followed by daily administration of vehicle (DSS + VEC, $n = 6$) for 5 days, and *4*) fed 1.75% DSS for 5 days followed by daily administration of LY411,575 (DSS + LY, $n = 6$) for 5 days. The whole body weights of mice were measured everyday. They were euthanized 12 h after the final administration. Colonic tissues were subjected to hematoxylin and eosin staining and analyzed by histological scoring following the criteria described elsewhere (21). Flow cytometry of thymocytes and splenocytes were performed as previously described (35, 41).

Immunoblot analysis. Immunoblots were performed as described elsewhere (18). The primary antibodies used were anti-Cleaved Notch1 (1:1,000, Cell Signaling Technology), anti-Hes1 (1:4,000, a kind gift from Dr. T. Sudo), and anti-β-actin (1:5,000, Sigma). Proteins were visualized either by the ECL Advance Western Blotting Kit (GE Healthcare) or ECL Western Blotting Kit (GE Healthcare).

Cell culture. The cell cultures and transfections of plasmid DNA were performed as described elsewhere (18). The inhibition of Notch signaling was achieved by the addition of LY411,575 (1 μM), synthesized according to Wu et al. (38). A cell line expressing Notch1 intracellular domain (Tet-On NICD1 cells) under the control of tetracycline or doxycycline (DOX, 100 ng/ml, Clontech) was generated as described elsewhere (18), using LS174T cells as parent cells. The cell lines were supplemented with Blastcidin (7.5 μg/ml, Invitrogen) and Zeocin (750 μg/ml, Invitrogen) for their maintenance.

RT-PCR assays. RT-PCR was performed as described elsewhere (18). Quantitative analyses using the SYBR green master mix (Qiagen) was performed by ABI 7500 (Applied Biosystems). Primer sequences for human β-actin, G3PDH, or MUC2 have been previously described (30). The primer sequences for other genes are summarized in Table 1. The results are shown as the means of the data collected from two rounds of assays, with each assay performed in triplicate. The data were statistically analyzed with paired Student's *t*-tests.

Human intestinal tissue specimens. Human tissue specimens were obtained from patients who underwent surgery for the treatment of Crohn's disease, UC, or colon cancer at Yokohama Municipal General Hospital or Tokyo Medical and Dental University Hospital. Written informed consent was obtained from each patient, and the study was approved by the ethics committee of Yokohama Municipal General Hospital and Tokyo Medical and Dental University.

Immunohistochemistry. Immunohistochemistry using intestinal tissues has been described elsewhere (12). The same antibodies used in immunoblot analysis were also used for the immunohistological staining of NICD1 and Hes1. The other antibodies used were anti-human Ki-67 (1:50, MIB-1, DAKO), anti-human PLA2G2A (1:200, sc-14468, Santa Cruz Biotechnology), anti-human MUC2 (1:100, Ccp58, Santa Cruz Biotechnology), and anti-mouse Ki-67 (1:50, TEC-3, DAKO). Microwave treatment (500 W, 10 min) in 10 mM citrate buffer was required for staining human tissues in Hes1, Ki-67, and NICD1 and for staining mice tissues in Ki-67. The tyramide signal amplification (Molecular Probes) was used for immunofluorescent detection of NICD1. Staining was visualized by an avidin-biotin-peroxidase complex (ABC) elite kit (Vector) using diaminobenzidine as a substrate or by secondary antibodies conjugated with Alexa-594 or Alexa-488 (Molecular Probes). The quantification of Hes1 (Fig. 1*B*), Alcian blue, Ki-67, or NICD1 (Fig. 8*B*) was conducted by the examination of nine randomly selected longitudinal sections of crypts selected from at least three different individuals. The data were statistically analyzed with paired Student's *t*-tests.

Microarray. Microarray analysis was performed using the Acegene human oligo chip 30K subset A (Hitachi software). Total RNA was collected before and after 24 h of NICD1 expression in LS174T cells and labeled using the Amino Aryll Message Amp aRNA kit (Ambion). The complete dataset of the analysis has been submitted to the NCBI Gene Expression Omnibus (GEO) and is accessible through GEO accession number GSE10136.

Table 1. *Primers used in the present study*

Gene	Primer Sequence	
	Forward	Reverse
Human Hes1	5′- ATGCCAGCTGATATAATGGAG -3′	5′- TCACCTCGTTCATGCAGTCG -3′
Human Notch1	5′- CCGAACGAATACAACCCTCT -3′	5′- GCGATCTGGGACTGCTGCATGCT -3′
Human PLA2G2A	5′- ACCATGAAGACCCTCCTACTG -3′	5′- GAAGAGGGGACTCAGCAACG -3′
Mouse Hes1	5′- TCAACACGACACCGGACAAACC -3′	5′- GGTACTTCCCCAACACGCTCG -3′
Mouse MUC2	5′- TCCACCATGGGGCTGCCACT -3′	5′- GGCCCGAGAGTAGACCTTGG -3′
Mouse TNF-α	5′- CTACTGGCGGTGCCAAGGCTGT -3′	5′- GCCATGAGGTCCACCACCCTG -3′
Mouse IFN-γ	5′- ACACTGCATCTTGGCTTTGC -3′	5′- CGGATGAGCTCATTGAATGCT -3′
MouseIL-1α	5′- CCCGTCCTTAAAGCTGTCTG -3′	5′- AATTGGAATCCAGGGGAAAC -3′
Mouse IL-1β	5′- TTGACGGACCCCAAAAGAT -3′	5′- GAAGCTGGATGCTCTCATCTG -3′
Mouse IL-6	5′- GCTACCAAACTGGATATAATCAGGA -3′	5′- CCAGGTAGCTATGGTACTCCAGAA -3′
Mouse PLA2G2A	5′- AAGAAGCCCAAATGCTGAAA -3′	5′- TTTATCACCGGGAAACTTGG -3′
Mouse β-actin	5′- CCTAAGGCCAACCGTGAAAAG -3′	5′- TCTTCATGGTGCTAGGAGCCA -3′

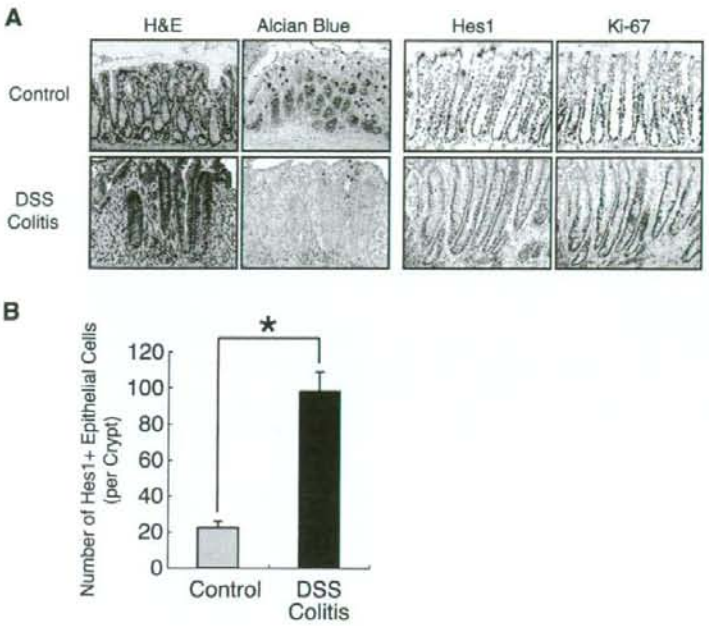

Fig. 1. Activation of Notch signaling is increased in crypts of dextran sodium sulfate (DSS)-induced colitis. *A*: histological analysis of DSS-induced colitis showing a decrease in mucin-producing intestinal epithelial cells (IECs) and an increase in Hes1- and Ki-67-expressing IECs within the crypts of the colitic mucosa. Blue staining with Alcian blue represents mucin production, whereas brown staining with diaminobenzidine (DAB) shows positive staining for Hes1 or Ki-67 (original magnification ×400). *B*: quantitative analysis of Hes1-positive IECs in crypts of normal or colitic mucosa. Data are shown as number of Hes1-positive cells per crypt on the basis of the analysis of immunohistochemical stainings. Error bars represent SD. $*P < 0.05$ on the Student's *t*-test. H & E, hematoxylin and eosin.

Plasmids. Hes1p-Luc, containing six tandem-repeats of the RBP-Jk binding site, was a kind gift from Dr. Kageyama (Kyoto, Japan). PLA2-Luc was generated by cloning a 2778-bp sequence 5′ of the human PLA2G2A gene (corresponding to −2,758 to + 20 of the promoter region) into a pGL3 basic vector (Promega). MUC2-Luc (40) was a kind gift from Dr. Yuasa (Tokyo, Japan). Tetracycline-dependent expression of NICD1 was achieved by cloning the gene encoding the intracellular portion of the mouse Notch1 (amino acid 1,704-2,531) into the pcDNA4/TO/myc-his vector (Invitrogen). All constructs were confirmed by DNA sequencing.

Immunostaining of cultured cells. Staining of cultured cells has been previously described (30). Detection of the MUC2 antibody was carried out either by the standard ABC method or by the Alexa 594-conjugated secondary antibody (Molecular Probes). The quantification of cells positive for MUC2 staining was performed by examining six randomly selected fields (three fields each in two individual counts) under ×400 magnification. The data were statistically analyzed with paired Student's *t*-tests.

ELISA. For PLA2G2A protein quantification, 1×10^6 cells were cultured in 2 ml of medium with or without DOX and analyzed with the human-PLA2 enzyme immunoassay kit (Cayman Chemicals). The incorporation of BrdU was examined by seeding cells at various cell densities in the 96-well plate, supplemented with DMSO or LY411,575. The BrdU was added 8 h before the end of culture, and the cells were subjected to analysis with the cell proliferation ELISA kit (Roche Diagnostics). The results are shown as the means of data collected by two rounds of assays, with each assay performed in triplicate. The data were statistically analyzed with paired Student's *t*-tests.

Reporter assays. The reporter assay was performed as previously described (18). Each assay was performed in triplicate, and the results were normalized using the *Renilla* luciferase activity. The results are shown as the means of normalized arbitrary units, and the data were statistically analyzed with paired Student's *t*-tests.

RESULTS

Hes1 is expressed in crypt epithelial cells of DSS-colitis. Since previous studies have evaluated the contribution of Notch signaling in the maintenance of mice intestinal epithelium (28, 33, 34), we sought to examine the role of Notch signaling in mice colitis. At first, we analyzed the expression of Hes1, a direct target gene of Notch, in mice with colitis induced by the oral administration of DSS (DSS-colitis, Fig. 1*A*). In the normal colon, crypts are predominantly composed of mature goblet cells that produce mucin. In such crypts, Hes1 is expressed in IECs residing at the lowest part of the crypt, which is also where Ki-67-positive IECs are found. In sharp contrast, the clear loss of mucin production was observed in the inflamed mucosa of DSS-colitis mice. The expressions of both Hes1 and Ki-67 were observed in a larger population of IECs, which were distributed from the bottom to the most upper regions of the crypt, suggesting that Notch signaling was activated in these IECs. The quantitative analysis of the immunostaining revealed significant increases in Hes1-positive IECs within the crypts of the DSS-colitis mice (Fig. 1*B*). These findings suggested that Notch signaling is activated in a greater number of IECs in DSS-colitis, which might be closely related with the greater number of proliferating IECs and the loss of mucin-producing IECs.

LY411,575 inhibits Notch activation and promotes goblet cell differentiation in mice intestine. To further examine the role of Notch signaling in colitis, we used LY411,575, a γ-secretase inhibitor (GSI) that is known to block Notch activation in vivo (14, 27, 36). Oral administration of LY411,575 for 5 consecutive days significantly reduced the expression of

Hes1 mRNA in mice intestine, suggesting that Notch activation was inhibited (Fig. 2*A*). In contrast, the expression of MUC2 mRNA was significantly increased by LY411,575, suggesting that the number of goblet cells increased. Consistent with this, histological analysis showed marked increases in mucus-producing IECs in the intestines of the LY411,575-treated mice (Fig. 2*C*). Consistent with reports from previous studies (27, 36), these results showed that LY411,575 could

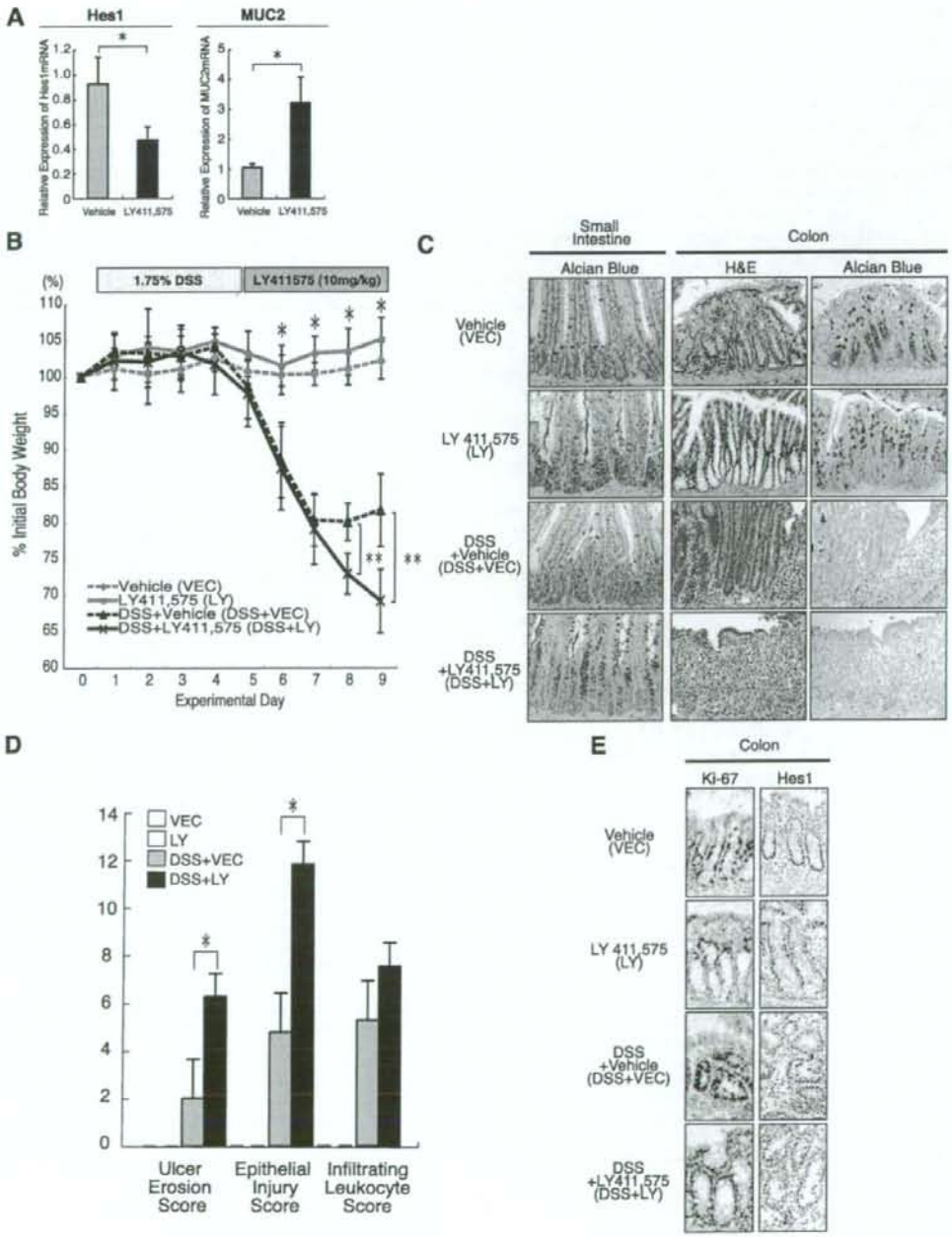

simultaneously inhibit Notch activation and promote differentiation to goblet cells in the mice intestine.

We also found marked atrophy of the thymus in LY411,575-treated mice (Supplemental Fig. S1*A*). Supplemental data for this article are available on the *American Journal of Physiology Gastrointestinal and Liver Physiology* website. Further analysis of the thymus revealed that the total number of thymocytes was significantly reduced (Supplemental Fig. S1*B*) and that the tissue architecture was disrupted (Supplemental Fig. S1*C*). Analysis of CD4/CD8 expression revealed a significant proportional reduction in double-positive cells (Supplemental Fig. S1*D*) and a reduction in the absolute number of cells (Supplemental Fig. S1*E*), suggesting that there was a significant loss of immature cells in the thymus with LY411,575 treatment. However, such an effect of LY411,575 was not present in the spleen (Supplemental Fig. S1, *A–E*). These findings clearly showed that the LY411,575 treatment had a systemic effect, affecting the thymus in addition to the intestine.

LY411,575 exacerbates DSS-colitis by impairing epithelial regeneration. Using the methods described, we designed an experiment to examine the effect of Notch inhibition during colitis (Fig. 2*B*). Mice were separated into four groups: vehicle alone (VEC), LY411,575 alone (LY), DSS with vehicle (DSS + VEC), and DSS with LY411,575 (DSS + LY). As of *day 5*, the total body weights showed significant reductions from *day 0* in DSS-treated mice (Fig. 2*B*) compared with the weights of those without DSS (the day when DSS treatment was started is designated as *day 0*). However, the DSS + LY mice showed even greater reductions in weight as of *day 8*; their reductions in body weight were significantly greater than the weight reductions in DSS + VEC mice (Fig. 2*B*). This severe loss of body weight observed in DSS + LY mice was also fatal because two mice in this group were dead at the time of euthanasia (fatality rate = 2/6, 33.3%). No deaths were observed in any other experimental group. These results suggested that LY411,575 significantly exacerbates the clinical course of DSS-colitis. A histological analysis of LY or DSS + LY mice showed a marked increase in goblet cells in the small intestine, confirming the effect of LY411,575 treatment (Fig. 2*C*). The increase in goblet cells was also observed in the colon of LY mice. A histological analysis of DSS + VEC mice showed a clear induction of colitis, as shown by the marked increase in inflammatory cells and the elongation of goblet cell depleted crypts. However, in sharp contrast, DSS + LY mice showed a severe loss of the epithelial layer in addition to an infiltration of inflammatory cells, which appeared to lack signs of epithelial regeneration (Fig. 2*C*). A histological scoring of the colonic tissues revealed increased ulcer formation and epithelial injury in DSS + LY mice compared with DSS + VEC mice, whereas no significant changes were observed in the degree of inflammation (Fig. 2*D*). Consistent with this, the mRNA expression of proinflammatory cytokines was increased in the colon of DSS-treated mice, but no clear differences were observed between DSS + VEC and DSS + LY mice (Supplemental Fig. S2).

For further analysis, we examined the expression of Hes1 and Ki-67 in the inflamed region of the colonic tissues. An increase in Hes1- or Ki-67-positive IECs was confirmed in DSS + VEC mice (Fig. 2*E*). However, both Hes1 and Ki-67 expression appeared to be markedly lost in the colonic crypts upon LY411,575 treatment (Fig. 2*E*). These results indicated that LY411,575 inhibits Notch activation and promotes goblet cell differentiation but also strongly inhibits proliferation of IECs, leading to a poor regenerative response and a severe exacerbation of DSS-colitis.

LY411,575 promotes goblet cell differentiation but inhibits proliferation of IECs in vitro. Previous in vivo results suggested that Notch activation might play critical roles in both the differentiation and proliferation of IECs. We further examined the in vitro effect of LY411,575 upon human colonic epithelial cell lines LS174T and HT29. As shown by the immunoblot analysis, the endogenous expression of both NICD1 and Hes1 was completely inhibited within LS174T cells by LY411,575 treatment (Fig. 3*A*). Consistent with this, RT-PCR analysis showed a marked decrease in Hes1 mRNA expression with LY411,575, which was maintained for up to 72 h (Fig. 3*B*). These data confirmed that LY411,575 could directly inhibit the activation of Notch within IECs.

Under this condition, we examined whether LY411,575 could promote goblet cell differentiation in vitro. Quantitative RT-PCR analysis showed a significant increase in MUC2 mRNA expression with LY411,575 treatment in both LS174T and HT29 cells (Fig. 3*C*). Consistent with this, a marked induction of MUC2 protein expression was observed in both of the cell lines that were treated with LY411,575 (Fig. 3*D*, red signal), resulting in a significant increase in the MUC2-positive cell population (Fig. 3*E*). The Alcian blue staining also showed a marked increase in mucin-producing cells in both cell lines with LY411,575 (Fig. 3*F*, black arrow). However, LY411,575 appeared to inhibit the proliferation of both cell lines since the incorporation of BrdU was significantly downregulated by LY411,575 (Fig. 3*G*). These results collectively showed that LY411,575 could directly inhibit Notch activation in IECs, which might subsequently promote goblet cell differentiation but also inhibit cell proliferation.

Activation of Notch1 suppresses goblet cell phenotype, but upregulates PLA2G2A secretion in human IECs. To further analyze the function of Notch activation in IECs, we gen-

Fig. 2. Inhibition of Notch activation by LY411,575 exacerbates DSS-colitis by impairing epithelial regeneration. *A*: LY411,575 suppresses Hes1 expression but also promotes MUC2 expression in mice intestine. After oral administration of LY411,575 or vehicle alone for 5 consecutive days, the small intestinal tissues of mice were subjected to quantitative RT-PCR analysis. Results from 3 mice in each group. Error bars represent SD. $*P < 0.05$ on the Student's *t*-test. *B*: LY411,575 significantly exacerbated wasting disease caused by DSS. As described in MATERIALS AND METHODS, mice were separated into 4 groups, and the body weight of each mouse was monitored throughout the experimental period. Error bars represent SD. $*P < 0.05$ for the difference between mice that were DSS treated (DSS + VEC and DSS + LY) or not treated (VEC and LY). $**P < 0.05$ for the difference between DSS + VEC and DSS + LY mice on the Student's *t*-test. *C*: LY411,575 exacerbated epithelial injury of DSS-colitis. Intestinal tissues of mice shown in *B* were subjected to histological analysis. Blue staining with Alcian blue represents mucin production (original magnification ×400). *D*: LY411,575 had no significant effect on inflammation of DSS-colitis. Histological scoring of colonic tissues obtained from each mice group is shown. Error bars represent SD. $*P < 0.05$ on the Student's *t*-test. *E*: LY411,575 inhibited proliferation of IECs via downregulation of Notch activity. Colonic tissues of mice were subjected to immunohistochemical staining for Hes1 and Ki-67. A less inflamed region was chosen for analysis of DSS + LY mice because the most inflamed region showed complete loss of the epithelial layer. Note that IECs expressing Hes1 or Ki-67 were confined within a narrow region of the colonic crypt in mice treated with LY411,575 (LY and DSS + LY).

erated a subline of LS174T cells (Tet-On NICD1 cells), in which forced expression of NICD1 could be induced in a tetracycline- or DOX-dependent manner. Immunoblot analysis of Tet-On NICD1 cells showed a clear induction of NICD1 and a subsequent increase in Hes1, with DOX addition (Fig. 4*A*). Consistent with this, the reporter activity of Hes1p-Luc was significantly upregulated with the induction of NICD1 in Tet-On NICD1 cells, indicating that there was an upregulation of the transcriptional activity of the Hes1 gene (Fig. 4*B*). These results confirmed that Tet-On NICD1 cells could express the functional NICD1 protein with DOX addition.

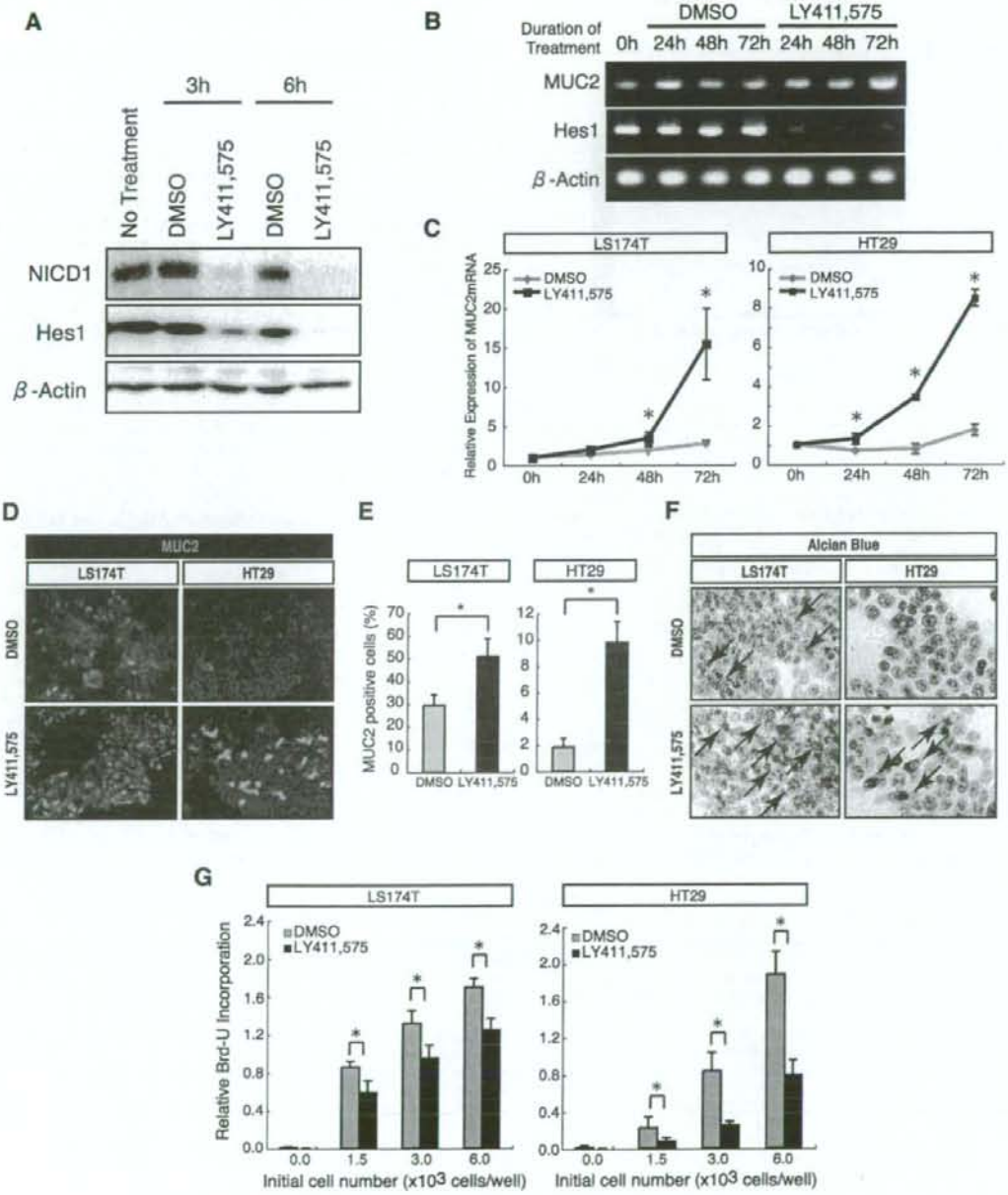

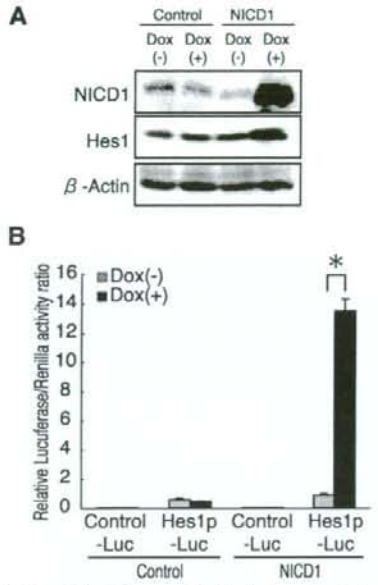

Fig. 4. Activation of Notch1 upregulates Hes1 expression in human IECs. *A*: establishment of a subline of LS174T cells expressing NICD1 under control of a tetracycline-dependent promoter (Tet-On NICD1 cells, designated as NICD1). Immunoblot analysis of Tet-On NICD1 cells showed a clear upregulation of both NICD1 and Hes1 expression with doxycycline (DOX) addition, whereas parental cells (designated as Control) remain unchanged. A low-sensitivity substrate (ECL) was used for visualization. *B*: transcriptional activity of Hes1 was upregulated with the expression of NICD1. Transcriptional activities of Hes1 gene in Tet-On NICD1 cells or control cells were analyzed by luciferase reporter assays using Hes1p-Luc. A reporter plasmid containing only the core-promoter of chicken β-actin gene served as a control (Control-Luc). Luciferase activities were measured after 12 h of culture with or without DOX. Error bars represent SD. $*P < 0.05$ on the Student's *t*-test.

Using this cell line, we found that the upregulation of NICD1 expression in LS174T cells significantly downregulated MUC2 mRNA expression (Fig. 5*A*). Further analysis with a microarray identified a group of genes that were up- or downregulated with NICD1 expression (Supplemental Tables 1 and 2). Among these genes, we focused on PLA2G2A, a gene expressed by Paneth cells, as it showed the most significant induction with NICD1 expression. Quantitative RT-PCR confirmed an upregulation of PLA2G2A mRNA expression with the NICD1 expression (Fig. 5*A*). Consistent with this, although the MUC2 protein expression was markedly suppressed (Fig. 5*B*), with resulting significant decreases in MUC2-positive cells (Fig. 5*C*) and mucin-producing cells (Fig. 5*D*), the PLA2G2A secretion was upregulated with NICD1 expression (Fig. 5*E*). These changes appeared to be regulated at the transcriptional level since the reporter activities of MUC2-Luc and PLA2-Luc showed a significant decrease and increase, respectively, with NICD1 expression (Fig. 5*F*). These results showed that, although the activation of Notch1 within LS174T cells suppressed goblet cell phenotype, it also upregulated the secretion of PLA2G2A, suggesting that the activation of Notch1 might surprisingly promote the acquisition of the specific functions of Paneth cells.

Notch1 is activated in crypt epithelial cells of the human intestine. Since we found that Notch signaling might regulate cell proliferation, goblet cell differentiation, and Paneth cell-specific function within IECs, we sought to clarify its relevance in human intestinal diseases. We first examined whether components of the Notch signaling pathway are expressed in the human intestine. An RT-PCR analysis of human intestinal tissues or epithelial cell lines successfully detected mRNAs of both Notch1 and Hes1 (Fig. 6*A*). The immunohistochemistry for NICD1 and Hes1 revealed that these proteins are expressed in the nuclei of crypt IECs (Fig. 6*B*). Similar to our observations in mice, the distribution of NICD1-positive or Hes1-positive IECs corresponded to that of Ki-67-positive IECs (Fig. 6*B*). Also, a magnified view of the staining showed a positive staining of NICD1 in columnar-shaped IECs and Paneth cells (Fig. 6*B*, black arrow) but not in goblet-shaped IECs (Fig. 6*B*, red arrowhead). Double staining of MUC2 and NICD1 confirmed the lack of NICD1 expression in goblet cells (Fig. 7*A*), whereas double staining of PLA2G2A and NICD1 confirmed expression of NICD1 in Paneth cells (Fig. 7B). These results strongly suggested that the NICD1 might function in vivo in the human intestine in a similar manner as was revealed in the in vitro study.

Increased activation of Notch1 is observed in the mucosa of UC. UC is one of the major forms of inflammatory bowel diseases, characterized by the persistent inflammation and ulcer formation in the colon. In the active region of UC, a loss of goblet cells, an ectopic expression of Paneth cell genes, and an increase in IEC proliferation are all known to be common pathological findings (7, 8, 13, 23). Thus our results strongly suggested that all of these pathological findings in UC might be mediated by the activation of Notch1 in IECs. We performed

Fig. 3. Inhibition of Notch activation promotes differentiation of goblet cells but suppresses proliferation of human IECs. *A*: LY411,575 downregulated expression of Notch1 intracellular domain (NICD1) and Hes1 in LS174T cells. Immunoblot analysis of LS174T cells treated with LY411,575 showing downregulation of endogenous NICD1 and Hes1 expression within 6 h from treatment. Cells treated with DMSO alone served as control. A high-sensitivity substrate (ECL Advance) was used for visualization. *B*: LY411,575 upregulated expression of MUC2 in LS174T cells. LS174T cells were subjected to semiquantitative RT-PCR analysis after treatment with either LY411,575 or DMSO. Note that expression of Hes1 was markedly decreased, whereas expression of MUC2 was increased after 72 h of treatment with LY411,575. *C*: LY411,575 significantly increased expression of MUC2 mRNA in both LS174T and HT29 cells. Cells were subjected to quantitative RT-PCR analysis after 0, 24, 48, and 72 h of treatment with either LY411,575 or DMSO. Error bars represent SD. $*P < 0.05$ for the difference between DMSO and LY411,575 treatment at the same time points on the Student's *t*-test. *D*: LY411,575 induced expression of MUC2 protein (red) in LS174T and HT29 cells. Cells were subjected to immunofluorescent staining of MUC2 after 72 h of treatment with either LY411,575 or DMSO (original magnification ×200). *E*: LY411,575 significantly increased the MUC2-positive cell populations among LS174T and HT29 cells. Quantitative analysis of *D* is shown by percent of MUC2-positive cells within total nucleated cells. Error bars represent SD. $*P < 0.05$, on the Student's *t*-test. *F*: LY411,575 induced mucin production in LS174T and HT29 cells. Cells were subjected to Alcian blue staining (black arrow) after 72 h of treatment with either LY411,575 or DMSO (original magnification ×400). *G*: LY411,575 significantly downregulated proliferation of LS174T and HT29 cells. A significant decrease in BrdU incorporation was observed with LY411,575 treatment in LS174T and HT29 cells. Incorporation of BrdU was measured by ELISA. Results are shown as arbitrary units of relative BrdU incorporation. Error bars represent SD. $*P < 0.05$ on the Student's *t*-test.

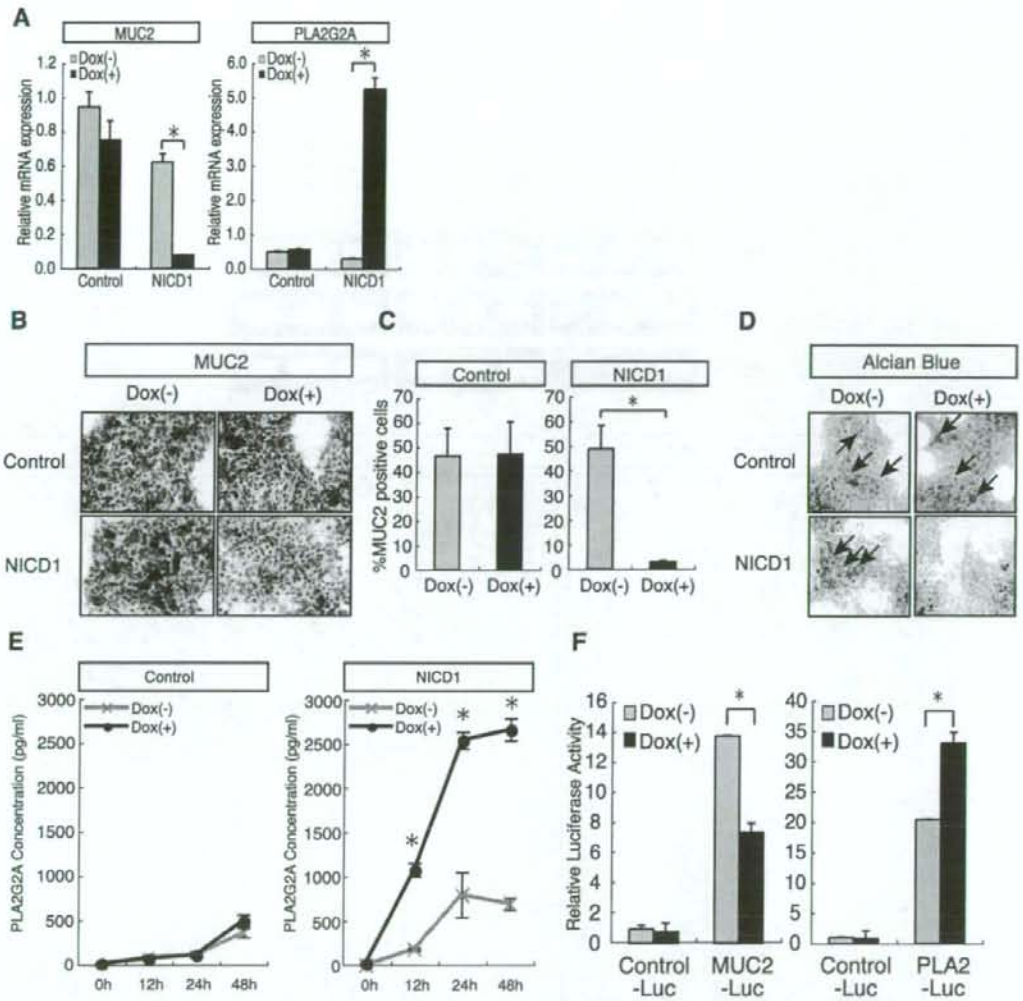

Fig. 5. Activation of Notch1 suppresses goblet cell differentiation but promotes expression of PLA2G2A of human IECs. *A*: expression of NICD1 in LS174T cells downregulated the expression of MUC2 but upregulated the expression of PLA2G2A. Quantitative RT-PCR analysis of MUC2 and PLA2G2A expression in Tet-On NICD1 cells and control cells is shown. Cells were subjected to analysis after 48 h of culture with or without DOX. Error bars represent SD. $*P < 0.05$ on the Student's *t*-test. *B*: expression of NICD1 in LS174T cells downregulated MUC2 protein expression. Tet-On NICD1 cells or control cells were subjected to immunostaining of MUC2 after 48 h of culture with or without DOX. Brown staining with DAB showed positive staining for MUC2 (original magnification ×200). *C*: expression of NICD1 in LS174T cells significantly reduced the number of cells expressing MUC2. Quantitative analysis of immunostaining shown in *B* is shown. Number of cells positively stained for MUC2 was counted and shown as percent of total nucleated cells. Error bars represent SD. $*P < 0.05$ on the Student's *t*-test. *D*: expression of NICD1 suppressed mucin production by LS174T cells. Tet-On NICD1 cells or control cells were treated as described in *B* and subjected to Alcian blue staining. The blue staining represents mucin-producing cells. (black arrow, original magnification ×800). *E*: expression of NICD1 upregulated PLA2G2A secretion of LS174T cells. Tet-On NICD1 cells or control cells were cultured with or without DOX, and culture supernatants collected at various time points were subjected to quantification of PLA2G2A using ELISA. Error bars represent SD. $*P < 0.05$ compared between DOX (+) and DOX (-) on the Student's *t*-test. *F*: expression of NICD1 in LS174T cells downregulated transcriptional activity of MUC2 gene but upregulated transcriptional activity of PLA2G2A gene. Transcriptional activity of MUC2 gene and PLA2G2A gene were measured by luciferase reporter assays using MUC2-Luc and PLA2-Luc as a reporter plasmid, respectively. pGL3-basic served as a control (Control-Luc). Luciferase activities in Tet-On NICD1 cells were analyzed after 12 h of culture with or without DOX. Error bars represent SD. $*P < 0.05$ on the Student's *t*-test.

histological analysis and found that in the crypts of UC, mucin production is markedly decreased (Fig. 8*A*, *top*, blue), whereas the number of Ki-67-expressing cells are markedly increased, distributing from the bottom to the uppermost part of the crypt (Fig. 8*A*, *bottom*, brown). In such crypts, NICD1-expressing cells showed the same distribution as Ki-67-expressing cells (Fig. 8*A*, *middle*, brown), suggesting that Notch1 is activated in an expanded proliferating cell population within the crypts of

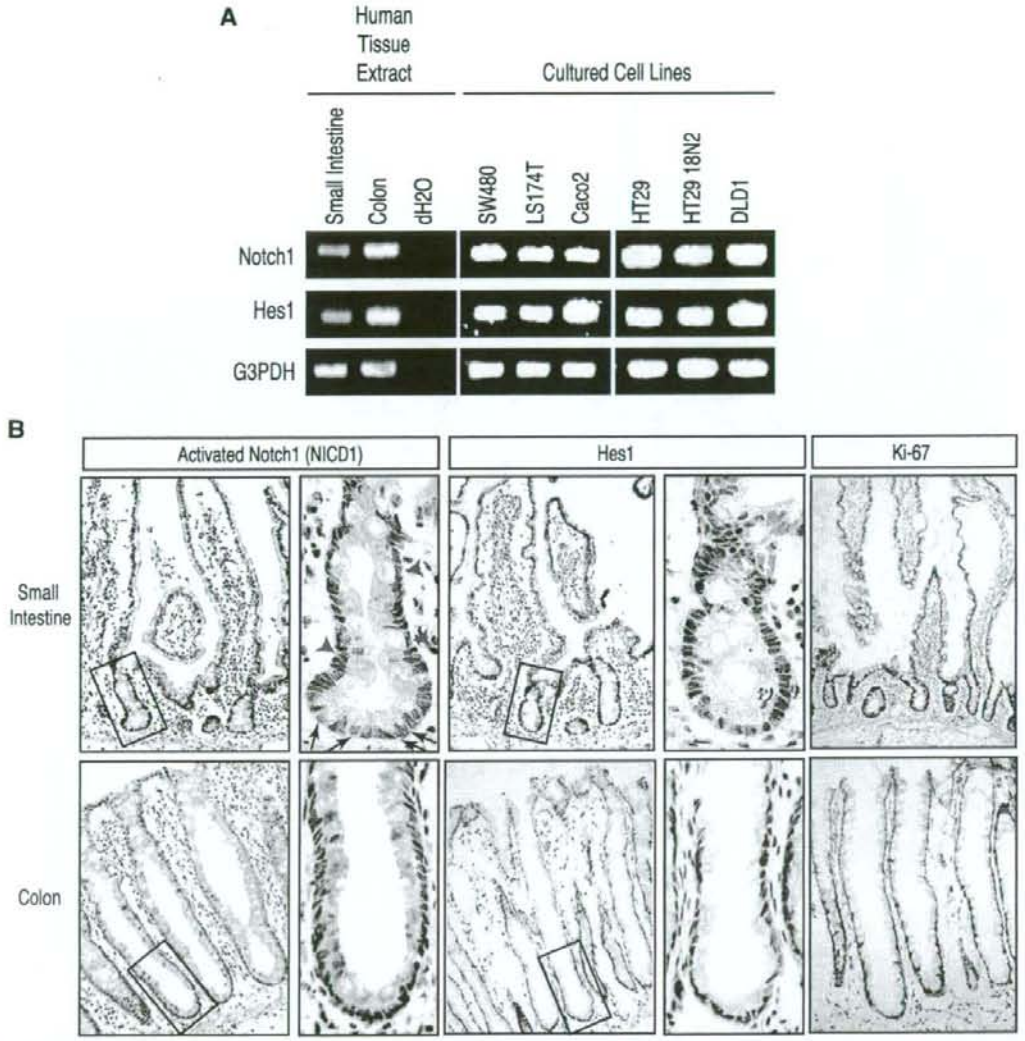

Fig. 6. Notch signaling is activated in crypt epithelial cells of the human intestine. *A*: RT-PCR analysis of human intestinal tissues and human intestinal epithelial cell lines. Expression of both Notch1 and Hes1 are clearly detected in all the examined tissues and cell lines. *B*: immunostaining of human intestinal tissues showing expression of NICD1, Hes1, and Ki-67. Brown staining with DAB showed positive results for NICD1, Hes1, and Ki-67 (original magnification ×200). Magnified view of the squared area is shown in the right side of the original picture (original magnification ×1000). Black arrows show Paneth cells clearly containing granules in the cytoplasm showing positive staining for NICD1, whereas red arrowheads show goblet-shaped cells lacking NICD1 staining.

UC. A quantitative analysis revealed that the number of IECs expressing NICD1 or Ki-67 per crypt is significantly increased, whereas the number of IECs producing mucin is significantly decreased in the crypts of UC (Fig. 8*B*).

We also looked for IECs expressing PLA2G2A within the colonic crypts. There was no expression of PLA2G2A in the crypts of the normal colon (Fig. 9*A*). However, an ectopic expression of PLA2G2A was clearly found in the crypts of the colon epithelia with UC (Fig. 9*B*). Our histological analysis revealed that Notch1 is clearly activated in such IECs ectopically expressing PLA2G2A (Fig. 9, *C* and *D*). Such activation of Notch1 in PLA2G2A-expressing cells could also be found in less inflamed regions of UC where there were fewer PLA2G2A-expressing IECs (Fig. 9, *E* and *F*).

From these results, we confirmed that Notch1 is activated in a greater number of crypt IECs in UC, presumably mediating goblet cell depletion, cell proliferation, and ectopic expression of PLA2G2A. We suggest that such Notch1-mediated changes

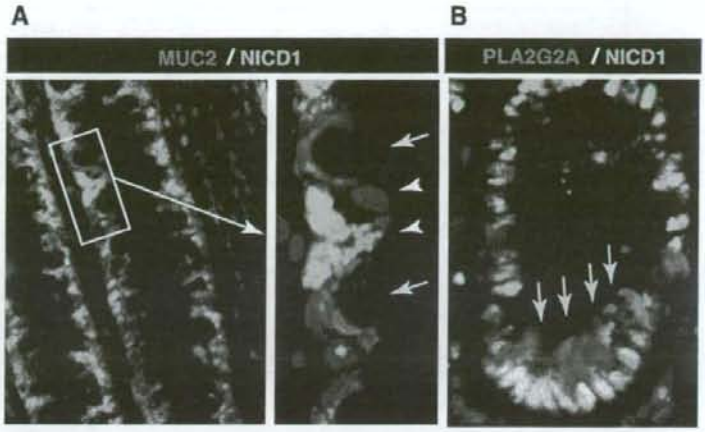

Fig. 7. Human Notch1 is not activated in IECs expressing MUC2 but is activated in IECs expressing PLA2G2A. *A*: human Notch1 was not activated in IECs expressing MUC2 in vivo. Double staining for MUC2 (red) and NICD1 (green) using human colonic tissue is shown. NICD1 and MUC2 were expressed in distinct populations of epithelial cells (*left*, ×400). A magnified view (*right*, ×1600) clearly shows cytoplasmic staining of MUC2 in goblet-shaped cells (yellow arrow), whereas nuclear staining of NICD1 in columnar-shaped cells (white arrowhead). *B*: human Notch1 is activated in IECs expressing PLA2G2A in vivo. Double staining for PLA2G2A (red) and NICD1 (green) using a human small intestinal tissue is shown. NICD1 and PLA2G2A were coexpressed in IECs residing at the lowest part of the crypt, suggesting activation of Notch1 in Paneth cells (yellow arrow, original magnification ×1000).

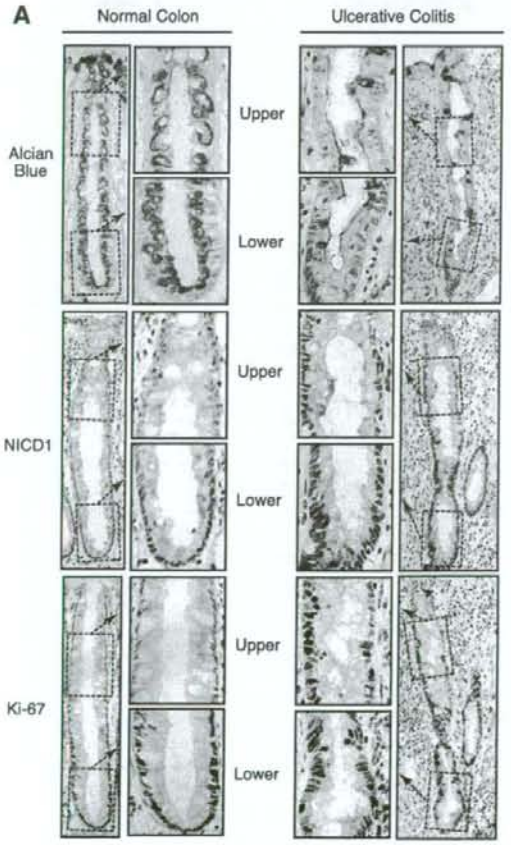

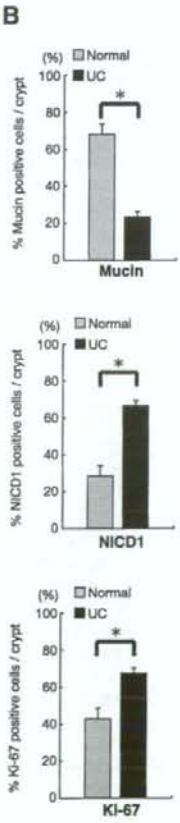

Fig. 8. Increased activation of Notch1 is observed in the crypts of patients with ulcerative colitis (UC). *A*: decreased expression of mucin and increased expression of both NICD1 and Ki-67 were observed in crypts of patients with UC. Mucin expression was examined by Alcian blue staining, whereas expression of NICD1 or Ki-67 was examined by immunohistochemistry with the use of human colonic tissues. Inner column shows magnified view of the upper (Upper) and lower (Lower) crypt areas identified by dashed line in the outer column. A marked decrease in Alcian blue-positive IECs is observed in a crypt of a patient with UC (*top*). In contrast, a marked increase in IECs expressing NICD1 (brown, *middle*) or Ki-67 (brown, *bottom*) was observed in patients with UC. Distribution of IECs expressing NICD1 or Ki-67 was restricted to the lower part of the crypt in normal colon, but it extended to the most upper region of the crypt in UC (original magnification, outer column ×400, inner column ×1600). *B*: significant decrease in IECs expressing mucin and significant increase in IECs expressing NICD1 or Ki-67 were observed in crypts of patients with UC. Quantitative analysis of the histological staining for mucin, NICD1, and Ki-67 is shown. Number of IECs positive for Alcian blue staining or immunohistochemical staining for NICD1 and Ki-67, respectively, were counted per crypt and normalized by total number of IECs. Results are shown as percent positive IECs per crypt. Error bars represent SD. $^*P < 0.05$ on the Student's *t*-test.

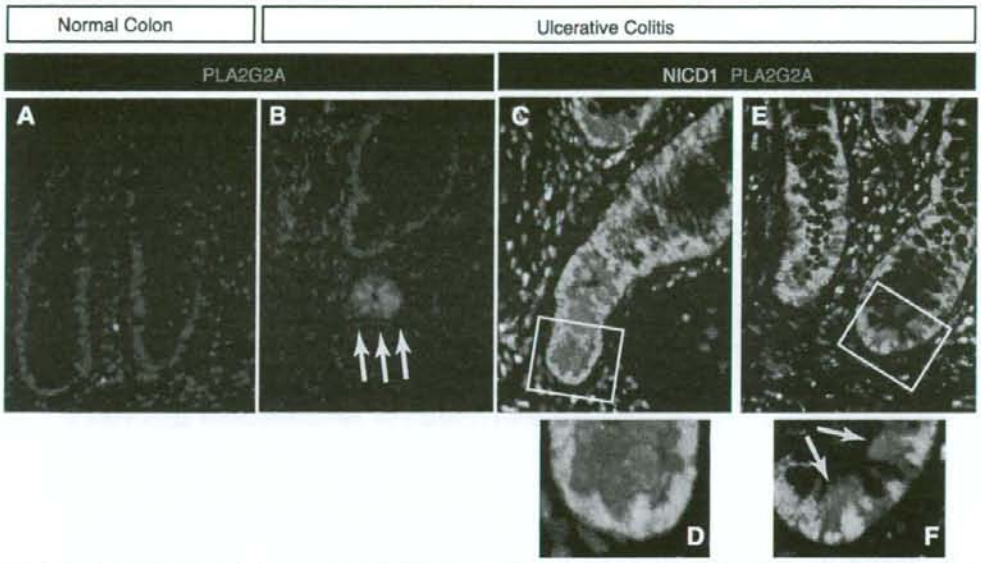

Fig. 9. Notch1 is activated in IECs ectopically expressing PLA2G2A. Fluorescent immunostaining for PLA2G2A (red) was completely negative in the crypts of normal colon (*A*, original magnification ×400), whereas some of the IECs in the crypts of a patient with UC were clearly positive for PLA2G2A (*B*, yellow arrow, original magnification ×400). Some cells in the lamina propria were also positive for PLA2G2A. Double immunostaining for NICD1 (green) and PLA2G2A (red) showed coexpression of NICD1 and PLA2G2A by colonic IECs of a patient with UC (*C–F*). In the inflamed region (*C*, *D*), NICD1 was expressed in most parts of the crypt IECs, and some proportion of those IECs coexpressed PLA2G2A (*C*, original magnification ×400). A magnified view (*D*, original magnification ×1000) of the indicated region (white square in *C*) clearly showed a nuclear distribution of NICD1 and a cytoplasmic distribution of PLA2G2A. In a less inflamed region, few IECs appeared to be positive for both NICD1 and PLA2G2A (*E*, original magnification ×400). Magnified view of the indicated region (white square in *E*) confirms coexpression of NICD1 and PLA2G2A in the nucleus and cytoplasm of an IEC, respectively (*F*, yellow arrow, original magnification ×1000).

observed in the mucosa of UC are not detrimental changes contributing to the persistence of the disease, but rather they are positive responses that help to regenerate the damaged epithelia, thereby aggressively contributing to the termination and recovery from the disease.

DISCUSSION

To date, several studies using knockout mice have revealed various functions of Notch signaling in IECs; one critical function is that of regulating the cell fates of IECs (31). The recent model accepted in such studies implicates Notch activation as a positive regulator of absorptive cell differentiation but a negative regulator of the differentiation of secretory lineage cells, including goblet cells. However, studies have suggested that Notch activation not only acts to determine the cell fates of progenitor IECs, but it may also regulate the number of proliferating populations within the crypt (6, 28, 33). Our results are consistent with the previous observations, and they further highlight the critical role of Notch activation in a situation when the rapid expansion of IECs is required (e.g., during the regeneration process in UC). Since the in vivo phenotype of Notch inhibition showed not only the loss of absorptive lineage cells but also the loss of the entire epithelial layer, this suggested that the activation of Notch may contribute to the expansion of both absorptive and secretory precursor cells and even stem cells. This is consistent with the observation by Vooijs et al. (34) that IECs that matured into absorptive cells must have also experienced Notch activation during development from the stem cell. Thus our results demonstrated the importance of Notch activation in the expansion of multilineage precursor IECs, whose function becomes critically required when tissue damage is present. In contrast, although Notch activation was predominant in the proliferating IECs of the colitic mucosa, its role in postmitotic IECs might be of less importance (42).

A recent study has shown that the chronic inhibition of Notch activation using LY411,575 (for up to 15 consecutive days) could impair the development of lymphoid cells (14, 36). Thus it may be possible that such an effect of LY411,575 might have altered the local immune function of the DSS-treated mice and thereby exacerbated their colitis. Indeed, LY411,575 proved to have a systemic effect, especially on the development of thymocytes (Supplemental Fig. S1). However, no effect was observed on splenocytes (Supplemental Fig. S1). Also, no effect was observed on local production of proinflammatory cytokines (Supplemental Fig. S2). Thus, although it is possible that LY411,575 might have some effect on the inflammatory response, its involvement on the exacerbation of the present colitis model may be minimal.

Also, GSI has been reported to promote the differentiation and inhibit proliferation of mice intestinal adenoma through the inhibition of Notch activation (33). Therefore, GSIs have been reported to have an antitumor effect (32). However, our results showed that the effects of GSIs may not be specific for tumor